Zeitschrift: IABSE reports = Rapports AIPC = IVBH Berichte
Band: 999 (1997)

Rubrik: Joints between structural members

Behaviour and Design of Composite Connections

David NETHERCOT
Head of Civil Engineering
University of Nottingham
Nottingham, UK

David Nethercot, born 1946 holds BSc, PhD & DSc degrees from the University of Wales. He is active in research on steel and composite construction and is currently chairman of IABSE WC2.

Summary

Previous experimental and numerical investigations of the use of composite action in beam to column joints in multi-storey frames are used as the basis for establishing a set of design procedures covering the key performance requirements of strength, stiffness and rotation capacity. The link between achievable levels of connection performance and the use of moment redistribution based design methods for non-sway composite frames has also been studied so that supply and demand may be balanced in achieving appropriate overall frame solutions.

1 Introduction

A major innovation in recently published structural design codes is the deliberate drawing together of the approach to be used when assessing the distribution of internal forces within a structure and the performance requirements of the connections. As an example, both EC3 and EC4 recognise the semi rigid and/or partial strength nature of many practical types of joint through the concept of the semi-continuous approach to frame design. This requires that explicit consideration be given to actual joint properties. Recognising the best description of joint behaviour to be its moment-rotation or M-ϕ curve, the key descriptions of this are defined as:

- Moment capacity M_c
- Initial rotational stiffness K_I
- Rotation capacity ϕ_u

The recent progress at Nottingham in first identifying the main governing influences on these properties and then in deriving methods for their prediction for a range of connection types forms the core of this paper. The presentation is restricted to non-sway frames since almost no data currently exists on the behaviour of composite connections subject to loading that places the slab in compression.

2 Investigations

Four interlinking techniques have been used to study the overall and detailed behaviour of composite connections:

- Examination of available test data
- Laboratory tests
- Numerical modelling
- Application of basic mechanics

All available composite connection test results have been collected together, carefully reviewed and placed in a computerised database. Specific tests, initially designed to simply investigate the inherent levels of composite action typically provided but normally neglected in design, and later aimed at both developing a better understanding of the complex force transfer mechanism and providing detailed load histories against which to validate numerical approaches have been conducted.

The development of a validated ABAQUS based model (1) for composite connections has permitted several of the more detailed and initially puzzling aspects of behaviour e.g. moment / shear (2) and moment / column axial load interaction (3), to be investigated. Interpreting the findings with the aid of some basic concepts in mechanics has led to the establishment of a unified design approach that provides good predictions for M_c, K_i and ϕ_u.

3 Moment Capacity M_c

Before attempting to devise a comprehensive design basis it is necessary to identify all the possible failure modes. Fig. 1, which shows these for a cleated arrangement, illustrates the importance of recognising the role of each of the components and the possibilities that when acting in combination forms of failure that might not be possible for the non-composite equivalent may occur. The next, and most important, step consists of deciding upon the mechanism of force transfer through the various components. Fig. 2 shows how this is accomplished for a finplate or web cleat arrangement (4). It should, however, be noted that several variants of this are possible, depending on the precise geometry, number of bolts, degree of reinforcement etc. The governing shear resistance may then be determined as the least of all potential shear resistances e.g. for a finplate six conditions must be considered:

i Shear resistance of the bolt group.
ii Bearing of the bolts against the finplate or beam web.
iii Weld resistance in shear.
iv Block shear failure of the beam web.
v Block shear failure of the finplate.
vi Equilibrium of the internal forces.

Explicit formulae for these and for the equivalent conditions for angle cleats and endplate (5) arrangements have been derived. From Fig.1 it is also necessary to check for overstressing of the beam web and column web. Item vi above is used to ensure that a consistent and achievable set of forces is finally used to calculate the moment capacity from:

$$M_c = P_v x$$

in which P_v = attainable connection shear
x = shear span

This approach has been fully validated using both the complete set of all appropriate test data and the supplementary numerical results

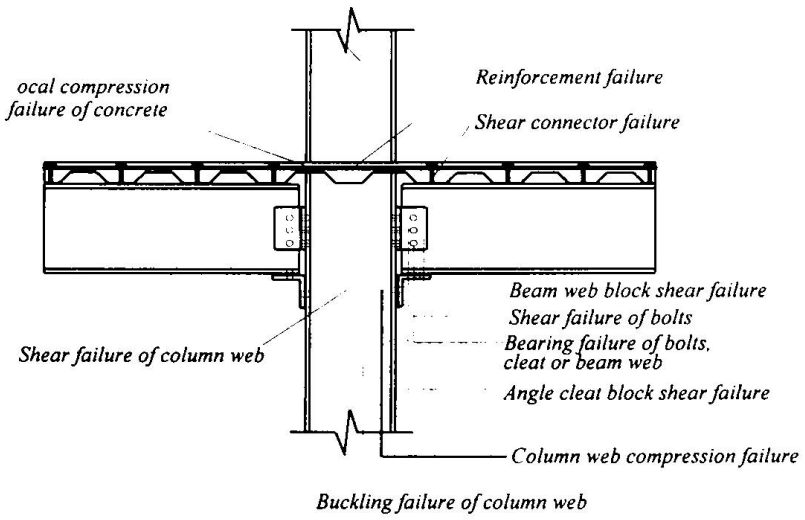

Figure 1. Composite angle cleated connection with possible failure modes

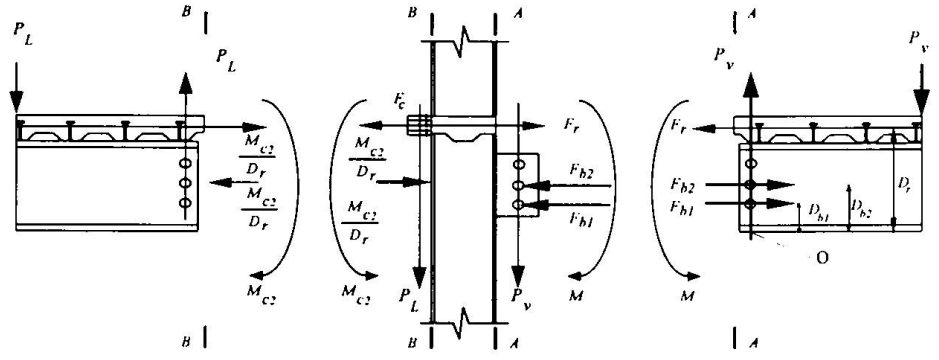

Figure 2. Free body diagram of the connecting parts showing internal forces (finplate connection and cleated connection with web cleats only)

4 Initial Stiffness K_c

Since both finplate and cleated arrangements involve the occurance of slip at uncertain stages due to the use of (normally) untorqued bolts in clearance holes subject to shearing action, accurate stiffness prediction is impossible. However, for endplates the model of Fig. 3 may be used to derive an explicit expression for K_I in terms of the various component stiffnesses, values for which may be obtained by considering the basic behaviour of the particular component in question (6).

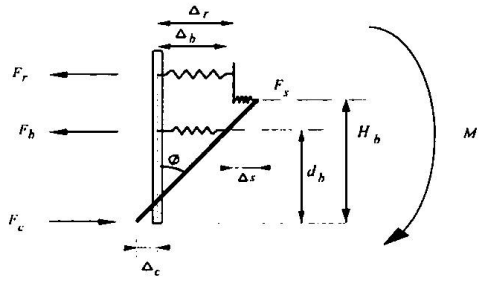

Figure 3. Spring model for initial stiffness of composite flush endplate connections

5 Rotation Capacity ϕ_u

Similarly, the model for predicting the available rotation capacity of endplate connections shown in Fig. 4 leads to an explicit expression for ϕ_u in terms of connection geometry and component stiffness (6). Although rather less reliable test data for both K_I and ϕ_u are available, comparisons against all thirtytwo suitable results show that both the above prediction methods give consistently good results.

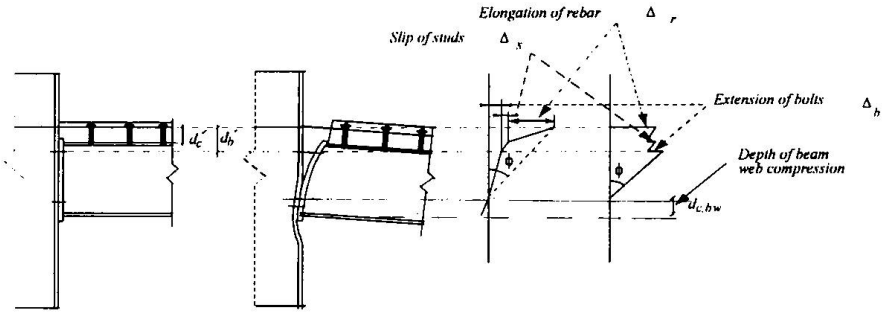

(a) (b) (c) (d)

(a) Connection before deformation
(b) Connection after deformation
(c) Deformation of components at connection face
(d) Representation of deformations for rotation calculation

Figure 4. Beam to column connection rotation capacity model

6 Frame Design

For strength design of non-sway composite frames the preferred approach uses the strong column / weak beam concept i.e. failure is controlled by collapse of the beams. Providing buckling effects are suppressed, collapse of any beam segment will occur by the formation of a 3-hinge mechanism. Possibilities for different levels of support moment (corresponding to different levels of M_c , including full beam capacity "fixed ends") are illustrated in Fig. 5. Examination of a wide variety of cases (7) has shown that the joints may be expected to reach their capacity before the mid-span region attains the sagging resistance of the composite section. Therefore formation of the final mechanism requires redistribution of moments from the supports to the span, a condition that necessitates some plastic rotation in the connections - hence the need to be able to predict ϕ_u.
Of the three potential limiting conditions:

i span moment reaches beam's sagging capacity
ii support moment reaches joint capacity
iii joint rotation reaches joint rotation capacity

the simplest design procedure corresponds to deliberately satisfying i & ii, whilst ensuring that iii is not violated. Studies show that since joint rotation and degree of moment redistribution are directly linked, iii may more easily be satisfied if the span moment is taken as less than the full sagging capacity (8,9). This additional design freedom is helpful in cases where the required joint rotation (for the formation of the mechanism of Fig. 5d) cannot easily be achieved by the preferred form of connection.

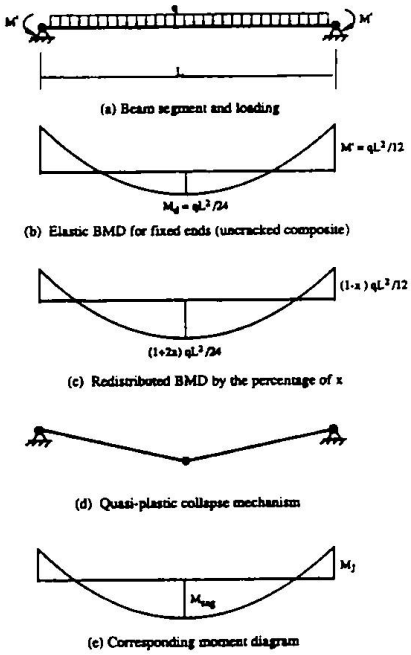

Figure 5. Moment redistribution and quasiplastic design

7 Conclusions

Recent research into the behaviour of composite beam to column connections, including their influence on the overall response of complete non-sway frames, has been reviewed. From this work a fully detailed design procedure has been developed.

8 Acknowledgements

This paper draws heavily upon the work of several of the author's colleagues at Nottingham, especially Drs B Ahmed and T Q Li. Financial support for the various research programmes has been provided by BRE, DTI, SCI and SERC.

9 References

1 Ahmed, B & Nethercot, D A., 'Numerical Modelling of Composite Flush Endplate Connections'. Journal of Singapore Structural Steel Society, Vol. 6, No. 1, 1995, pp. 87-102.

2 Ahmed, B & Nethercot, D A., 'Effect of High Shear on the Moment Capacity of Composite Cruciform Endplate Connections'. Journal of Constructional Steel Research (in press).

3 Ahmed, B & Nethercot, D A., 'Effect of Column Axial Load on Composite Connection Behaviour'. Structural Engineering Review (under review).

4 Ahmed, B., Li, T Q & Nethercot, D A., 'Design of Composite Finplate and Angle Cleated Connections'. Journal of Construction Steel Research (in press).

5 Ahmed, B & Nethercot, D A., 'Design of Composite Flush Endplate Connections'. The Structural Engineer (in press).

6 Ahmed, B & Nethercot, D A., 'Prediction of Initial Stiffness and Available Rotation Capacity of Major Axis Composite Flush Endplate Connections'. Journal of Constructional Steel Research (in press).

7 Li, T Q., Choo, B S., Nethercot, D A, 1995. 'Determination of Rotation Capacity Requirements for Steel and Composite Beams'. Journal of Constructional Steel Research, Vol. 32, No. 3, pp. 303-332.

8 Nethercot, D A, 1995. 'Semi-rigid Joint Action and the Design of Non-sway Composite Frames'. Engineering Structures, Vol. 17, No. 8, 1995, pp. 554-567.

9 Nethercot, D A., Li, T Q & Choo, B S, 1995. 'Required Rotations and Moment Redistribution for Composite Frames and Continuous Beams'. Journal of Constructional Steel Research, Vol. 35, 1995, pp. 121-163.

Ductile Steel-Concrete Composite Joints

Ali A. NAJAFI
formerly Research Assistant
University of Warwick
Coventry, UK

Ali Najafi, born 1958, received his degrees from the Universities of Tehran and Warwick. After practising structural engineering in Iran, and managing a construction company, he conducted research into composite construction. He is currently investigating computer-aided architectural and structural design at the University of Strathclyde.

David ANDERSON
Professor
University of Warwick
Coventry, UK

David Anderson, born 1944, received his degrees from the University of Manchester. His interests include the drafting and assessment of codes for steel and composite structures. He is Convenor of the Project Team for conversion of ENV1994-1-1 to a European Standard.

Summary

The paper treats the ductility requirements for partial-strength beam-to-column joints in composite construction. The slab reinforcement enhances the resistance of the joint but may limit the rotation capacity. The ductility needed to permit formation of a beam-type plastic hinge mechanism is examined and proposals are made for design. The sources of ductility in composite joints are also examined, and a method to predict the limiting rotation capacity of end-plate joints is demonstrated.

1. Introduction

Ductility is needed in continuous and semi-continuous construction if in-elastic methods are used for global analysis. These include approaches based on the attainment of a mechanism of plastic hinges. The need for ductility at hinge locations is expressed in terms of "rotation capacity", being the localised rotation to achieve the distribution of moments used in design. With partial-strength joints, the rotation must be accommodated by the joint itself, because it is components within the joint, rather than the adjacent members, which behave inelastically. Thus the rotation capacity of the joint becomes one of the key properties. For design, it is the capacity φ_{cd} available at the design moment resistance M_{cc} (Fig. 1). To deliver the necessary rotation capacity, some component(s) must yield in a dependable manner. For steelwork joints, appropriate components are plate elements in bending and column webs in shear.

Compared to bare steelwork, composite joints provide greater moment resistance; in a braced frame, through the tensile action of the slab reinforcement. However, they usually remain partial-strength relative to the composite beam, and tests show that the rotation capacity at the enhanced moment is reduced (Anderson (ed), 1997). The rotation capacity is curtailed by several possible modes of failure; some are peculiar to composite joints; others are more likely because the tensile action of the reinforcement increases the balancing compression around the bottom flange of the steel section, thereby encouraging buckling.

This paper examines the influence of failure modes on the rotation capacity of composite joints for braced frames, and indicates how this property can be predicted. The requirements though concern the rotation needed for the assumed distribution of moments. These needs are addressed first.

2. Required rotation capacity

2.1 Analysis methods

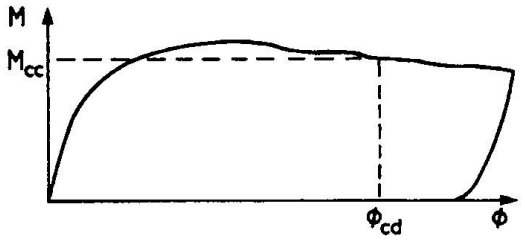

Fig. 1 :Rotation capacity

Numerical methods have been developed to determine the requirements (Najafi, 1992; Li et al, 1995). These were developed independently; comparison of results therefore strengthens confidence in both approaches and provides evidence to judge the appropriateness of simple plastic design for frames including partial-strength composite joints. The analysis due to Najafi is now outlined.

The analysis extends one by Johnson for fixed-ended composite beams, by including semi-rigid and/or partial-strength joints. Moment-curvature relationships for the beam's cross-section in hogging and sagging bending are determined from geometric data and material properties. An iterative procedure is then followed to determine a bending moment distribution which satisfies equilibrium and, through the moment-curvature relationships, ensures compatibility. The shear connection is assumed to provide full interaction, and plane sections are assumed to remain plane. The stress-strain curves for concrete in compression and reinforcement are as given in BS5400 (1978). To account for a proportion of load to be long-term, the concrete strains (except the final limiting strain) may be multiplied by a creep factor. Concrete in tension is assumed to crack and no account is taken of tension stiffening. If the slab is formed with profiled sheeting, the contributions of the decking and of concrete within the troughs are both neglected. The relation for structural steel is linear elastic-plastic, followed by strain-hardening at a modulus of E/33 once the strain exceeds eight times the yield value. To determine design values, the partial safety factors for concrete, reinforcement and structural steel were taken as 1.50, 1.15 and 1.0 respectively.

To obtain the moment-curvature relationships, values of curvature are varied. For each value, the position of the neutral axis is altered until equilibrium of direct forces is achieved; the moment is then calculated. The maximum value is taken to correspond to a limiting stress in the steel of 1.3 times the yield value or to a limiting concrete strain in compression of 0.0035.

To analyse a beam, values of end moment are varied. For each value, the distribution of bending moments is altered (whilst maintaining equilibrium relationships) until integration of the corresponding curvatures satisfies the condition of zero slope at mid-span. Equilibrium then determines the load level. Failure is assumed once a moment exceeds the maximum value for which moment-curvature data is available.

To account for end connections, the integration of curvatures includes an end rotation determined from the moment-rotation characteristic specified for the joint. If the characteristic has a plateau, then provided the mid-span region can resist further moment, the analysis continues by incrementing that moment. Equilibrium considerations and integration of curvatures lead to the corresponding connection rotation. The procedure permits reductions in increments as limiting conditions are approached, to determine the response with good accuracy.

The analysis distinguishes between propped and unpropped construction. In the former, no bending action is assumed until full interaction has been achieved. In the latter, account is taken of bending in the steel section. By specifying a stiffness for the steelwork connection, account is taken of semi-rigid joint action during construction.

2.2 Parametric studies

Those by Najafi covered the following ranges:

Beam span (L) : 6.0, 9.0 and 12.0m
Span : depth ratio (L/D) (based on depth of steel section) : 20 - 30
Steel sections : Universal Beams in S275 and S355 grades
Effective breadth of slab : Sagging region 0.175L
Hogging region 0.125L
Overall depth of slab : 120mm
Depth of decking : 46mm
Concrete : Cube strength 30 N/mm^2
Reinforcement : 1% of the effective area of concrete above decking; S460 grade.

The design resistance of the connection, M_{cc}, varied between 70% and 25% of the maximum design moment capable of being resisted by the composite beam in sagging bending, M_{pc}.

Propped and unpropped construction was considered.

2.3 Results

The following results were observed from the studies:

1. The rotation required to develop a beam-type mechanism was independent of the connection stiffness, provided that the first plastic hinge forms in the joint; this has been confirmed by Najafi using a graphical presentation and proved by Li using energy theorems.

2. Required rotation increased approximately linearly with reduction in M_{cc} (Fig. 2).

3. Increase in L/D from 20 to 30 caused the required rotation to rise by approximately 30%.

4. As plastification spreads in the mid-span region, the demands on rotation capacity increase sharply. Curve (i) in Fig. 2 shows the rotations required to develop the maximum sagging moment permitted by the analysis. If only 95% of this value is required, then the required rotation capacity is given by (ii). A reduction of at least 30% is obtained.

5. Compared with a uniformly-distributed load, the required rotation can increase by the order of 50% if point loads act at the one-third points.

6. The rotational requirements increase if unpropped construction is adopted.

2.4 Proposals for design

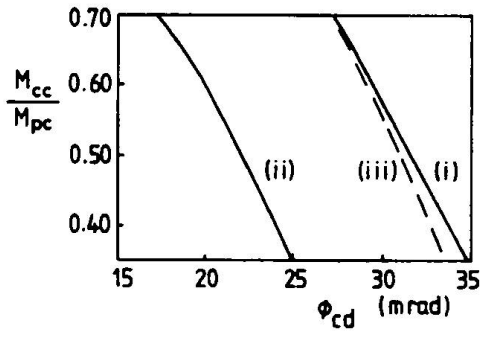

Fig. 2 : 305x165UB40 S355 9m span UDL (Propped construction)

As the required rotation capacity rises sharply if very extensive plastification is required at mid-span, it is appropriate to limit the sagging resistance moment in design to less than the maximum permitted. The sensitivity is shown not only by comparing curves (i) and (ii) in Fig. 2, but also by considering the results of Li et al (1996). The latter computed the maximum resistance moment by rectangular stress-block theory, as permitted by design codes. For the case examined in Fig. 2, the rotation capacity to obtain 95% of this value is shown by curve (iii). This corresponds closely to the present authors' results for the maximum moment - but the latter was determined by elastic-plastic analysis with the limitations given in (2.1).

An upper limit for the required rotation in propped construction can be determined from Fig. 2, which corresponds to the maximum L/D likely to be suitable in practice (Lawson and Gibbons, 1995) and to the highest steel grade in common use. For a uniformly-distributed load and a relative connection moment of 0.5, 22mrad is needed to attain a mid-span moment equal to 95% of the maximum permitted by the authors' analysis. By comparison with results by Li, this is equivalent to 90% of the resistance from BS5950 (1990) for the case shown. For point loads at one-third points, the requirement would be approximately 33mrad.

For unpropped construction, the requirements will depend on the relative load resisted while in this condition, and on whether simple or semi-continuous design is used for that stage. Preliminary studies indicate that the mid-span moment should be limited further, to the order of 85%, to limit rotation requirements to the above values.

3. Ductility available in composite joints

3.1 Failure modes

Possible modes include fracture of the reinforcement, loss of anchorage, failure of the shear connection, failure of the concrete slab by bearing or transverse splitting, and local buckling of steelwork. As for steel joints, some components must deform in a dependable manner to provide an assured rotation capacity. The likelihood of this can be judged from tests representative of composite joints envisaged in practice (Lawson and Gibbons, 1995).

Tests on joints with steel web and flange cleats have demonstrated the importance of slip between the cleats and the steel beam section (Altmann et al, 1991; Aribert et al, 1994; Davison et al, 1990; Xiao et al, 1994). The slip is erratic though and, when prevented, the ductility of the joint is compromised (Davison et al, 1990). A common failure mode was buckling of the column web in transverse compression. If loading continued, further rotation would occur but a significant reduction in moment could be experienced. The tests showed that with only welded mesh for reinforcement, fracture was likely at very limited rotations. In contrast, provision of high-yield reinforcing bars gave 28mrad before fracture, even though slip had been prevented (Davison et al).

With steel fin plates, Xiao et al (1994) have shown that composite joints can develop rotation capacities of over 40mrad. The steel connection derives flexibility from bolt deformation in shear and bolt hole distortions. However, such deformations are dependent on whether or not bolts slip into bearing and calculation of deformation is not straight-forward.

Xiao et al have also shown that joint rotations of the order of 40mrad can be achieved without substantial loss of moment, if partial-depth end plates are attached to the beam clear of the bottom flange. The capacity comes partly from the initial clearance between the lower part of the beam and the face of the column. The tests were terminated as buckling of the beam web was occurring. Although the rotation capacity could be regarded as adequate, the position of the end plate limits the resistance that can be developed.

In contrast, a joint with a full-depth ('flush') end plate maximises the lever arm for the tensile force in the reinforcement, and can provide a worthwhile stiffness during unpropped construction. Tests by Anderson and Najafi, Aribert et al and Xiao et al are taken as representative. This configuration lacks the slip deformations and distortion of bolt holes developed by other joint arrangements. In some tests the maximum recorded rotation was below 30mrad because loading ceased with the onset of buckling; fracture of the reinforcement did not then occur. Other tests showed that if column web buckling was prevented and the shear connection was ductile, rotation capacities of over 35mrad were achieved with a maximum of 1% high-yield reinforcement in the slab. Failure occurred by fracture of the reinforcement, or the tests were terminated at high deformations caused in part by substantial slip of the shear connection or by local buckling of the compression region of the beam. The likelihood of the latter is influenced by the tensile resistance that can be developed in the upper part of the steel connection; the use of thinner end plates or column flanges can lead to fracture of reinforcement occurring at a lower rotation due to a more limited balancing force causing buckling.

Provided that local buckling of the beam only occurs once the design moment resistance of the joint has been attained, these tests have shown that high rotations (> 40mrad) are achievable with only moderate reduction in peak resistance. However, the extent of buckling deformations is influenced by imperfections whose magnitudes are unknown to the designer. With slip of the steelwork connection and bolt-hole deformations excluded, either by the joint configuration or by the difficulty in ensuring these occur in a predictable manner, yielding of the reinforcement remains as the main source of predictable deformation capacity.

3.2 Rotation capacity due to deformation of the reinforcing bars

As composite joints may require substantial rotation capacity, it is important that the deformation of the reinforcing bars prior to fracture can be calculated. A method taking account of tension stiffening has recently been proposed (Anderson (ed), 1997). The results shown in Table 1 compare the proposal with three of the authors' tests (Anderson and Najafi, 1994) in which the only variable was the amount of reinforcement. The specimens were constructed propped. In the test designations, the figure(s) refers to the number of 12mm diameter high-yield bars included in the slab. The calculations are based on measured material properties. The additional rotations given in Table 1 relate to slip of the shear connection (Aribert, 1996) and an allowance for plastic compression in the beam flange immediately adjacent to the joint, where justified by the level of ultimate moment. In S8F and S12F the compressive force, required to balance the tensile action of the reinforcement and the bolts as the connection approached failure, exceeded the yield resistance of the flange by a substantial margin. It is assumed that the strain in the flange reached eight times the yield value (at which strain-hardening was taken to commence in (2.1) above) and that this remained constant over the distance of 130mm from the connection to the point along the beam at which the rotation was being measured.

	Rotation (mrad)				
Test	Rebars	Slip	Compression	Total	Experiment
S4F	20	5	-	25	27
S8F	24	6	4	34	36
S12F	26	8	4	38	55

Table 1: Predicted and measured rotation capacity

The calculated result for S4F includes allowance for mesh, whose contribution was significant in this lightly-reinforced specimen. Good agreement was obtained for this test and for S8F. The experimental rotation corresponded in both cases to fracture of the reinforcement. In S12F substantial deformation arose from local buckling of the bottom flange of the beam adjacent to the connection and the rebars did not fracture. The test was terminated at 55 mrad.

4. Conclusions

Composite connections with full-depth end plates provide a suitable configuration for beam-to-column joints. The moment resistance is substantial; this limits the demand for rotation capacity in plastic design. For the most critical load case expected in practice, a capacity of at least 33mrad should be provided. Using common grades of structural steel, this will permit 90% of the design sagging moment of resistance to be attained in a composite beam constructed as propped.

Tests have shown that such rotation capacity is readily obtainable, but is dependent partly on reinforcement of appropriate quality and quantity being provided. Calculation methods are available to determine these requirements. The resulting combinations of beam section and connections provide significant economies compared to nominally-pinned construction.

References

Altmann R, Maquoi R and Jaspart J-P, Experimental study of the non-linear behaviour of beam-to-column composite joints. *J Construct Steel Research* **18** (1991), 45-54.

Anderson D (ed) *Composite Steel-Concrete Joints in Braced Frames for Buildings.* COST-C1. European Commission Directorate-General XII, Brussels, 1997.

Anderson D and Najafi, A A, Performance of composite connections: major axis end plate joints. *J. Construct. Steel Research* **31** (1994), 31-57.

Aribert J-M, Lachal A, Muzeau J-P and Racher P, Recent tests on steel and composite connections in France. *Proceedings of the Second State of the Art Workshop* , COST-C1 European Commission Directorate-General XII, Brussels, 1994, 61-74.

Aribert J-M, Influence of slip of the shear connection on composite joint behaviour. *Connections in Steel Structures III* Pergamon, 1996, 11-22.

BS5400 Steel, Concrete and Composite Bridges Part 4 Code of practice for design of concrete bridges. BSI, London, 1978.

BS5950 Structural Use of Steelwork in Building Part 3 Section 3.1 Code of practice for design of simple and continuous composite construction. BSI, London, 1990.

Davison J B, Lam, D and Nethercot D A, Semi-rigid action of composite joints. *Struct. Engr.* **68** (1990), No. 24, 489-499.

Lawson R M and Gibbons C, *Moment connections in Composite Construction : Interim Guidance for End-Plate connections.* SCI, Ascot, 1995.

Li T Q, Choo B S and Nethercot D A , Determination of rotation capacity requirements for steel and composite beams. *J. Construct. Steel Research* **32** (1995),303 - 332

Li T Q, Ahmed B and Lawson R M , Required rotation of composite connections. *Report,* SCI, Ascot 1996.

Najafi A A, *End Plate Connections and their Influence on Steel and Composite Structures.* PhD Thesis, University of Warwick, 1992.

Xiao Y, Choo B S and Nethercot D A, Composite connections in steel and concrete I : Experimental behaviour of composite beam - column connections. *J. Construct. Steel Research* **31** (1994), 3 - 30.

Composite Joints - Further Experimental Results

Helmut BODE
Professor Dr.-Ing.
University Kaiserslautern
Kaiserslautern, Germany

Helmut Bode, born 1940 in Dresden, received his Ph. Degree at Bochum University. Since 1980 he is Professor of Civil Engineering at Kaiserslautern University, Germany.

Hans-Josef KRONENBERGER
Research Assistant
University Kaiserslautern
Kaiserslautern, Germany

Hans-Josef Kronenberger, born in 1961, got his civil engineering degree in 1990, followed by a year as a structural engineer, since 1991 his researches have been concerned with composite joints.

Werner MICHAELI
Research Assistant
University Kaiserslautern
Kaiserslautern, Germany

Werner Michaeli, born in 1966, received his Civil Engineering Degree in 1993, since this time he investigates the behaviour of composite joints.

Summary

The design of composite structures requires a classification system for the joints. Thus, it is necessary to calculate stiffness, moment resistance and ultimate rotation of the joints. If plastic design methods shall be used, the available ultimate rotation of the joint has to be compared with the rotation at the joint, required by the structure and its loading. In this paper the ultimate rotation of composite joints is investigated and described by means of selected test results. Possibilities to increase the ultimate rotation of the joint, which may be necessary for the required or full moment redistribution in the structure, will be lined out.

Introduction

Composite joints consist of a number of components transferring forces between the connected members, such as the steelwork connection, which in turn consists of several components, the reinforced concrete slab and the column web panel. All these components provide a particular, in general non-linear, force-deformation behaviour, thereby influencing the behaviour of the joint and the whole structure. Besides the structural detailing of the joint components, the arrangement within the structure and corresponding parameters as the shear connection between the steel beam and the slab, the loading and the method of erection have to be considered in order to describe the moment-rotation behaviour of the joint [1]. Tests on substructures as well as tests on components and large scale tests with semi-continuous composite structures have been carried out. The results from such tests can be used to calibrate models to determine the characteristic joint properties (the initial stiffness, the moment resistance and the rotation capacity).

Tests with composite joints and structures

During the last years more than 30 tests on symmetrically loaded composite joints and four tests on semi-continuous composite floor beam structures over two spans were carried out at Kaiserslautern University. Some results will be shown and discussed in this paper.

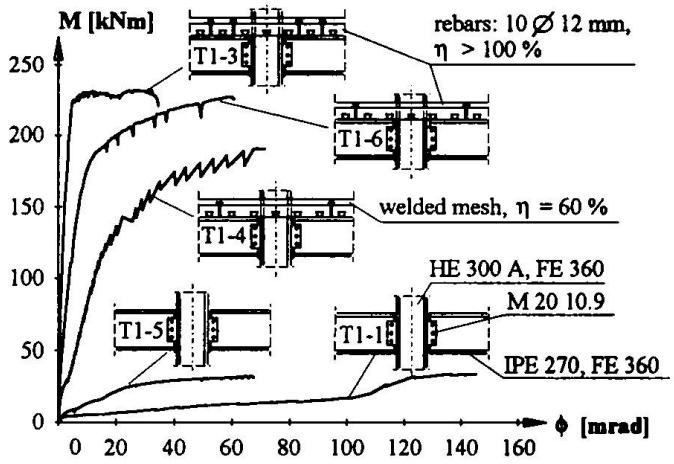

Fig. 1: Moment-rotation curves from tests with finplate connections [2]

In a series of tests with joints with finplate connections the influences from different components were investigated. Figure 1 shows achieved moment-rotation curves. In the tests on bare steel joints (T1-1 and T1-5) the influence of a contact plate between the lower beam flange and the column flange was investigated. The contact plate leads to a direct transfer of compression forces, thereby increasing stiffness and reducing ultimate rotation. In two other cruciform tests, the composite behaviour of the same steelwork connection, but with a continuous concrete flange was examined. In test T1-6 rebars with high ductility and full shear connection were used to increase stiffness and moment resistance of the joint. Partial shear connection however leads to a reduced stiffness and resistance, but increases the ultimate rotation as it can be seen from test T1-4, in which the same reinforcement ratio was provided as in test T1-6. This test indicates, that it might be possible to use welded mesh reinforcement in hogging bending areas, but only in combination with partial shear connection, which then provides the necessary ductility. In addition to these tests with cruciform specimens a large scale test with a composite floor beam over two spans with two point loads per span was carried out (T1-3). Full shear connection over the whole beam length was used. The joints at the interior support were the same as in test T1-6. Comparing the curves from tests T1-3 and T1-6 yields however opposite results. The differences are due to the acting width of the slab and the different arrangement of shear connectors. In test T1-6 the first shear connector was placed in the second rib of the steel sheet close to the joint, while in the beam test the first shear connector was located in the first rib.

In a further test series on composite joints with finplate connections the number of rebars was varied. Figure 2 shows the moment-rotation curves of these tests. A detailed description of these tests is given in [1, 3]. It was found that besides the stiffness and moment-resistance also the ultimate rotation is influenced by the reinforcement ratio, as it can be seen from the figure.

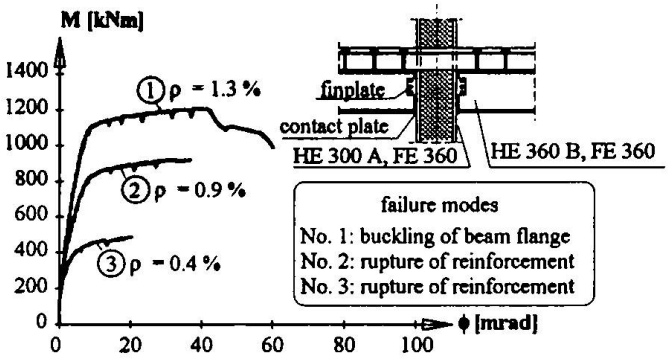

Fig. 2: Influence of reinforcement ratio on joint behaviour

Besides such tests on beam-to-column joints, beam-to-beam connections were also investigated. The considered boltless steel connection (Fig. 3) is an example for interconnected floor beams with the main beam underneath. Moment resistance was achieved by reinforcement in the slab and a contact plate between the lower steel flanges. In this test series the degree of shear connection and the arrangement of shear connectors were varied. A detailed description of these tests is given in [4, 5]. The tests show, that in comparison with full shear connection and uniformly distributed shear connectors along the whole beam length, partial shear connection (test S2-3) as well as a

certain distance between the first shear connector and the joint (test S2-4) reduce the stiffness, but increase the ultimate rotation of the joint.

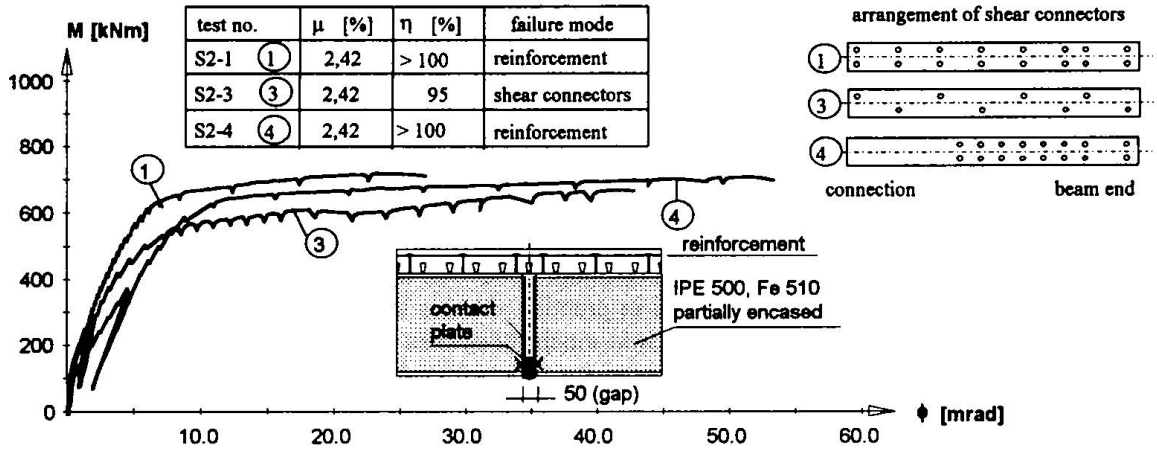

Fig. 3: Experimental moment-rotation curves

Figure 4 shows test results from a composite floor beam structure semi-continuous over two spans, which consisted of two simply supported steel beams and a continuous reinforced composite slab. Each beam was loaded at four points per span. At the interior support a boltless connection as in figure 3 was used. Continuity and moment resistance in negative bending were again achieved by ductile rebars in the slab and a contact plate between the lower steel flanges. Welded mesh provided some additional anti-crack reinforcement. Full shear connection along the whole beam length was provided by uniformly distributed shear connectors. The beams were propped during casting.

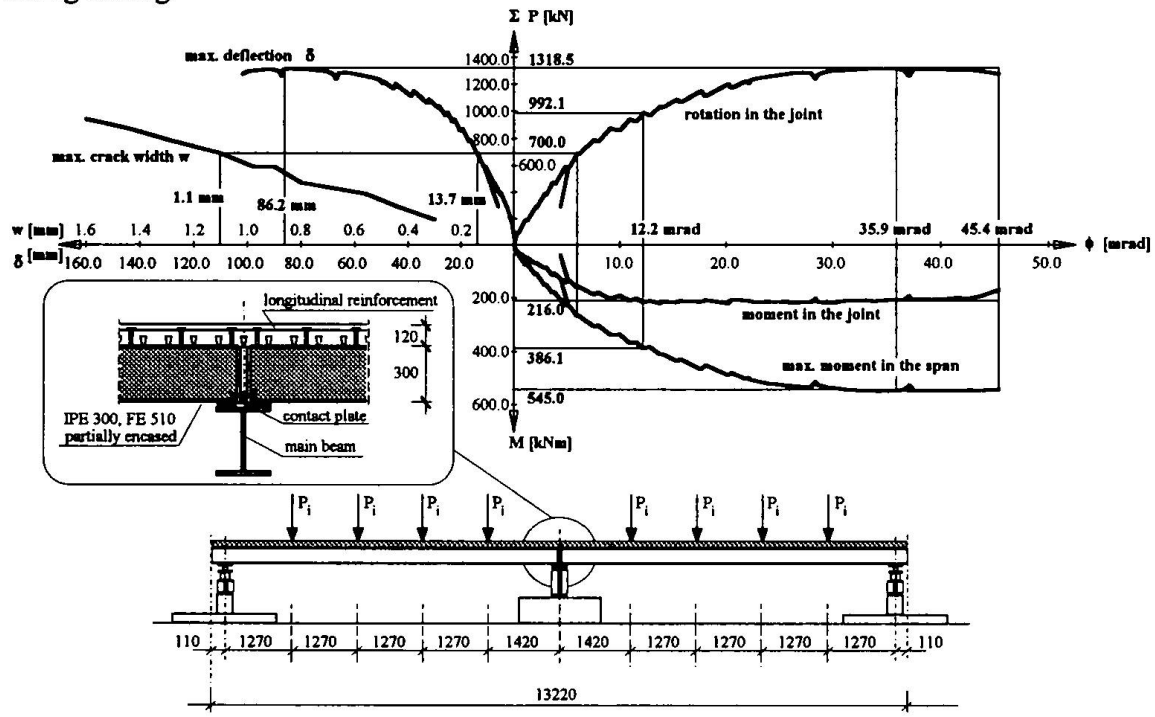

Fig. 4: Results from a test with a semi-continuous floor beam [5]

Figure No. 4 presents the full test information from this floor beam structure. The upper right diagram shows the applied load versus rotation in the joint at the interior support measured during

the test. The diagram below represents the moment development at the joint and in the span. At a rotation of about 12 mrad the joint reaches its plastic moment resistance while only 2/3 of the plastic moment resistance at midspan is achieved. From this rotation up to failure the joint behaves plastically. A rotation of about 36 mrad yields the full plastic moment resistance at midspan. The joint provides a higher rotation capacity than necessary, and failure of the structure due to rupture of the reinforcement occurs at a rotation of about 45 mrad. Thus, this part of the diagram shows that for this investigated test specimen rigid plastic analysis can be applied to calculate the ultimate load. The left diagram contains the deflection at midspan and the crack width at the interior support. From the obtained ultimate test load the load-level corresponding to the serviceability limit state was recalculated being approximately 700 kN. Up to this load the joint still shows a linear elastic behaviour. The corresponding maximum deflection at midspan was measured to be 13.7 mm, which is within the limits required in practice. At this load the maximum crack width however was measured being 1.1 mm, which is much more than the corresponding upper limit according to EC 4 [6], even though a reinforcement ratio of 1.54 % was used in the test specimen.

Ultimate rotation of composite joints

In [8] a method is described for the calculation of the ultimate rotation of a joint in cases where failure occurs in the tension zone of a joint. This procedure takes into account the deformations in the slab and at the steel concrete interface. In order to provide better results, it was enlarged by an additional factor taking into account some plastic deformations in the compression zone of the joint [9]. Thus, the ultimate rotation of a composite joint can be calculated by:

$$\phi_u = \frac{\Delta_{u,s} + s + \Delta_a}{D + D_r}, \qquad (1)$$

where $\Delta_{u,s}$ is the elongation of the reinforced concrete slab, s is the slip at the steel concrete interface close to the joint, Δ_a is the plastic deformation including buckling effects in the compression zone of the joint, D equals the height of the steel beam and D_r is the distance between the upper layer of reinforcement and the steel beam.

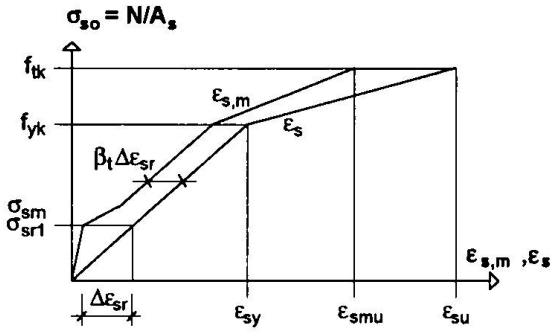

Fig. 5: Simplified stress-strain relationship of embedded reinforcing steel

The reinforced concrete slab is anchored to the steel beam by shear connectors, and its force-deformation behaviour differs from the behaviour of the reinforcement only. Figure 5 shows the simplified stress-strain relationship of embedded reinforcing steel together with the corresponding curve for reinforcement only as described in [10]. The embedded reinforcement curve provides a higher stiffness and a lower ductility than reinforcement alone (tension stiffening effect). Besides other parameters the properties of the reinforced concrete part depend mainly on the reinforcement ratio.

The ultimate average strain $\varepsilon_{s,m,u}$ of embedded reinforcement can be calculated as follows [10]:

$$\varepsilon_{s,m,u} = \varepsilon_{sy} - \beta_t \cdot \Delta\varepsilon + \delta \cdot \left(1 - \frac{\sigma_{sr1}}{f_{y,s}}\right) \cdot \left(\varepsilon_{su} - \varepsilon_{sy}\right), \qquad (2)$$

where β_t and δ are curve parameters. However, due to stress concentrations at the column flanges, this strain does not occur uniformly along the whole distance between the centreline of

the column and the first shear connector. This location of the first shear connector influences the strain distribution in addition, as it can be seen from the test in figure 3. Thus, in case of full interaction the ultimate elongation of the reinforced concrete slab can be calculated being

$$\Delta_{u,s} = L \cdot \varepsilon_{s,m,u} \qquad (2)$$

for $a \leq D_r$, with the distance L between the centreline of the column and the first shear connector and the distance a between the joint and the first shear connector or

$$\Delta_{u,s} = \left(\frac{h_c}{2} + D_r\right) \cdot \varepsilon_{s,m,u} + \varepsilon_{sy} \cdot (a - D_r) \qquad (3)$$

for $a > D_r$, and the depth h_c of the column section.

The improved method was used to calculate the ultimate rotations, measured in the tests outlined before and to compare them with test results, see table No.1. The agreement is excellent, although the amount of reinforcement, the degree of shear connection, the arrangement of the shear connectors and the type of test specimen (cruciform, large scale beam test over two span) were varied in these tests.

Test	ρ_s	η	$\phi_{u,test}$ [mrad]	$\phi_{u,calc}$ [mrad]	$\phi_{u,calc} / \phi_{u,test}$	figure	failure mode
S2-1	2.42 %	> 100 %	27,6	28,0	1,01	3	reinforcement
S2-2	1.45 %	> 100 %	24,5	24,7	1,01	-	reinforcement
S2-3	2.42 %	≅ 95 %	42,7	41,1	0,96	3	shear connectors
S2-4	2.42 %	> 100 %	53,2	54,4	1,02	3	reinforcement
S5-2	1.54 %	> 100 %	43,6	43,8	0,99	4	reinforcement
T1-3	0,88 %	> 100 %	33,8	35,8	1,06	1	reinforcement
T1-6	0,88 %	> 100 %	60,0	59,7	0,99	1	reinforcement
No. 1	1.30 %	> 100 %	43,5	44,8	1,03	2	beginn of buckling
No. 2	0.90 %	> 100 %	37,4	38,2	1,02	2	reinforcement
No. 3	0.40 %	> 100 %	18,9	17,9	0,95	2	reinforcement

Table 1: Comparison between measured and calculated ultimate rotation

It should be mentioned however, that this method provides correct results only if failure of the reinforcement or the shear connectors occurs. This method yields an upper limit for the ultimate rotation in cases, where the bolts in the steelwork connection fail or if local instabilities in the compression zone of the joint occur.

Conclusions

Equation (1) contains the main contributions to calculate the ultimate rotation with high accuracy if the realistic behaviour of reinforced concrete in negative bending and appropriate slab lengths are taken into account. Slip at the steel concrete interface as well as deformations due to local instabilities can also contribute to the ultimate rotation.

The detailing of joints and the adjacent beam sections is very important and can reduce or enlarge the ultimate rotation. Shear connectors placed close to the joint reduce the free elongation length of the slab. Such an arrangement increases stiffness, but reduces the ultimate rotation.

Partial shear connection in combination with ductile shear connectors and profiled steel sheeting enlarges the ultimate rotation of the joint, even if reinforcement of normal ductility (for example prefabricated welded mesh) is used.

Rigid plastic analysis has been applied to analyse the ultimate load of the tested floor beam structure over two spans. Large rotations in the joints are however necessary to make use of the high beam resistance in sagging moment areas. The required ultimate rotation of the joint can clearly be reduced, if the load carrying capacity is reduced to only 90 %. In case of the tested beam, such a reduction reduces the required rotation to about 50 % and this would lead to a required rotation capacity of about 2.

The use of partial strength joints together with rigid plastic analysis reduces the beam length in hogging bending. Thus, the contribution of the beam in negative bending to the required rotation (cracking of concrete and yielding of steel) is further reduced, while the contribution of the joint has to be increased.

The required rotation in the joint however can be further reduced by the loading history and type of erection. Unpropped construction together with simple steelwork joints and continuity in hogging bending areas only after the concrete has hardened reduces the required rotation of the composite joint in addition.

Acknowledgement

The work on this scientific research project has been supported by DFG (German Research Foundation). In addition it was sponsored by several German companies, which delivered material and structural elements for the test specimen. This support is gratefully acknowledged

References

[1] Bode, H., Kronenberger, H.-J.: Moment-Resisting Composite Joints, in *Composite steel-concrete joints in braced frames for buildings* (ed. D. Anderson), published by the European Commision, Brussels 1997

[2] Michaeli, W.: Zum Nachweis der Tragfähigkeit und Rotationskapazität von Verbundanschlüssen unter Berücksichtigung des Stabilitätsverhaltens, Ph.D. (in preparation), University of Kaiserslautern, Germany

[3] Bode, H., Ramm, W., Elz, S. Kronenberger, H.-J.: Composite Connections - Experimantal Results. *Semi-Rigid Structural Connections*, IABSE Colloquium Istanbul, 1996

[4] Bode, H., Kronenberger, H.-J.: Behaviour of Composite Joints and their Influence on Semi-Continuous Beams, Proceedings of the Engineering-Foundation Conference *Composite Construction III*, Irsee, 1996

[5] Kronenberger, H.-J.: Ein Beitrag zum Verhalten von Anschlüssen im Verbundbau unter besonderer Berücksichtigung von Nachgiebigkeiten in der Verbundfuge und des Einflusses der Herstellung. Ph.D. (in preparation), University of Kaiserslautern, Germany, 1997

[6] Eurocode 4, Part 1.1, CEN, 1992

[8] Aribert, J.-M.: Influence of Slip of the Shear Connection on Composite Joint Behaviour. Proceedings of the Third International Workshop on Connections in Steel Structures, ECCS and AISC, Trento, May 1995

[9] Anderson, D.: Technical paper No. AN/60 'Rotation capacity', COST-C1/ECCS-TC11 drafting group

[10] CEB-FIP Model Code 1990. Comité Euro-International du Beton, Lausanne, 1990

Modelling the Nodal Zone Behaviour in a Composite Frame

Claudio BERNUZZI
Research Associate
Univ. of Trento
Trento, Italy

Claudio Bernuzzi, born in 1962, received his engineering degree at the University of Pavia. He has been at the University of Trento since 1987 and his research work is focused on both steel and steel-concrete semi-continuous composite frames.

Shi Lin CHEN
Visiting Research Assoc.
Univ. of Trento
Trento, Italy

Shi Lin Chen, born in 1965, received his doctor degree at the Wuhan University of Hydro-electric Engineering. He has been a faculty member in Tsinghua University since 1991. He is engaged in the research about non-linear behaviour of structures.

Riccardo ZANDONINI
Professor
Univ. of Trento
Trento, Italy

Riccardo Zandonini, born in 1948, received his engineering degree at the Technical University of Milan, where he served as a faculty member from 1972 to 1986. He has been at the Faculty of Engineering in Trento since 1986. His research activity is devoted to the study of steel and steel-concrete composite structures.

Summary

Traditional design approaches for steel-concrete composite frames generally overlook the actual joint response and adopt simplified analysis models. Consequently, more refined design rules based on a complete understanding of the joint behaviour should be used in order to account for the relevant benefits associated with the semi-continuous frame model.
This paper deals with the nodal behaviour in composite frames. Key features of the nodal zone response are outlined, basic requirements for an accurate joint simulation are discussed and, finally, the preliminary results of an extensive numerical study are presented.

1. Introduction

Steel-concrete composite constructions represent very convenient solutions for civil and commercial buildings. Their design, which is generally based on ideal behavioural models (i.e., simple and rigid frame models), neglects the relevant benefits associated with composite joints action. As recently showed by several experimental and numerical studies [1-3], all joints possess flexural stiffness and moment capacity and the actual range of their behaviour is intermediate between the ideal model of simple and rigid joints. Hence, a reasonable use of the degree of continuity associated with the nodal zone improves the overall efficiency as well as the cost effectiveness of composite frames, especially when spans are long.
Despite the semi-continuous frame model is actually included into European Standard for composite structures [4], no specific recommendations are provided for their design, due to lack of fully validated approaches able to predict the semi-rigid behaviour of beam-to-column joints.
A study on joint action in steel-concrete composite systems is currently in progress at the University of Trento. On the basis of tests of composite cruciform joint specimens [5,6] as well as of full-scale sub-frames [7], the key phenomena and the related parameters influencing joint performance were identified. The study is now in the second phase, which is devoted to the development, validation and calibration of finite element (FE) models capable of simulating in an accurate way the joint response in composite frames. The FE modelling technique enables to single out the significant factors which influence the joint response; this is a necessary pre-requisite to the set up of simplified prediction procedures aimed to be used in design practice.

In this paper the key features of the nodal zone response of composite frames are summarised and the requirements for accurate FE models simulation are discussed. Finally, the preliminary results of an on-going numerical study on joints are presented.

2. Joint behaviour

A complete account of the behaviour of beam-to-column composite joints would need to recognize its three dimensional nature. However, the presence in composite framed systems of rather stiff continuous floor slab allows generally out-of-plane and torsional deformations of joint to be neglected. Moreover, with reference to in-plane behaviour, rotational flexibility appears as the most important characteristic affecting the global structural response. As a result, the joint behaviour can be accurately described by its in-plane moment-rotation (M-Φ) curve, for which, in case of joints under hogging moment, three branches can basically be identified: elastic (uncracked and cracked), inelastic (with progressive deterioration of stiffness) and plastic.
A feature peculiar of nodes in composite frames is that partial continuity may be sought between the beams and the column (as in steel frames), depending on the steel connection details as well as on the contact between the concrete slab and the column faces, or just between two adjacent beams, mainly due to the reinforcing bars of the slab across the column. Except that for joints to external columns, the complex problem of beam-to-column interaction, arising in case of unsymmetrically loaded nodes, may be practically neglected if the steel column is totally encased in the concrete slab [6].
As reported in [1], a significant number of variables play a substantial role in the development of joint action and hence affect the M-Φ curve. This relationship, which is the end product of a complex interaction in the nodal zone, depends on the key joint components and, in particular, on:

- the concrete slab: its axial stiffness in tension governs remarkably joint response in elastic uncracked phase. After cracks, slab merely serves to transfer tensile force to reinforcement with the aid of shear studs;
- the slab reinforcement: the amount of longitudinal rebars, which carry tensile force after attainment of tensile concrete strength, is the most important parameter affecting strength, rotational capacity and to some extent stiffness of the joint. Moreover, a proper design of transverse reinforcement is essential in order to active the strut mechanism involved in the horizontal shear transfer;
- the connection system between concrete slab and steel beam: stud distribution affects the cracking pattern whilst the degree of steel-concrete interaction influences significantly the joint response in its latest nonlinear phases, where slip and uplift of the slab can occur;
- the steel beam-to-column connection: non-negligible moment capacity (of the order of the negative plastic moment of the composite beam) may be achieved while maintaining simple details in the steel work, which transfer the compressive force from beam to column. Stronger connection typologies, such as end plate connections, improves remarkably the joint behaviour in the post-elastic phases, due to the transferring of tensile force also by means of the upper row of bolts. Non-linearities of this component, which can be caused by slippage, in case of cleated connection, as well as by changing of the contact zone of the compressive stresses, affect reasonably the M-Φ curve;
- the steel beam: bottom flange together with web transfer the compressive force to the column through the connection. Failure due to local buckling of the beam bottom flange does not lead to an immediate loss of resistance in semi-rigid joint as in rigid joint.
- the column: with reference to most common cases of joints framing into the column major axis, column web failure in shear as well as in compression, which affect substantially joint moment

resistance, can be prevented by means of web stiffener in case of H bare sections or of concrete encasement for composite columns.

The action of these key components on composite joints can be singled out from experimental analysis, which results nevertheless a costly approach and is essential to establish the fundamental background for the validation of all theoretical approaches. However, the experimental analysis has by its very nature a limited scope. Hence, the parametric investigations appear possible only by means of FE simulations, which enable for an exhaustive understanding of the joint behaviour and of the transfer force mechanisms between frame members and joints over a sufficiently extensive range of both mechanical and geometrical parameters.

3. Joint modelling

Although FE method has been successfully used to model steel beam-to-column joints [9], only a very limited number of studies [6,10-12] was focused on the FE analyses of composite nodes.

Despite an accurate simulation of the response of composite joints should require a three-dimensional (3D) analysis, two-dimensional (2D) models can be adopted in order to reduce the computation difficulties associated with large 3D meshes. In the case of a 2D representation, the contribution of the uncracked slab generally requires a preliminary 3D elastic analysis, which allows the relevant slab effective width to be defined[12,13].

Due to the complex interaction between the main nodal components as well as the key features of each of them, FE joint models should consider both geometrical and material non-linearity. As far as the material laws for steel components (beam, column, steel connection details, studs and rebars) are concerned, a good agreement with the actual behaviour is usually provided by the sole uniaxial multilinear stress-strain relationship, which can be correlated to a more complex and representative state of loading, via the selection of suitable yielding criterion (von Mises, Drucker-Prager, etc.). For the slab modelling, concrete constitutive laws provided by general purpose FE packages are based on a smeared-cracked approach, which assumes an equivalent isotropic continuum with smeared cracks for the simulation of the slab after the attainment of the concrete tensile resistance[14,15]. Due to the presence of longitudinal bars in the concrete slab, two modelling techniques can be adopted for the simulation of the slab reinforcements:

- a discrete rebar approach: rebars are modelled using truss or beam non-linear elements, which satisfy the displacement compatibility with the concrete elements;
- a smeared rebar approach, in which rebar-concrete interaction in tension can be modelled by appropriate modifications of the concrete constitutive relationship [15,20].

Moreover, an accurate simulation of the interaction (contact/separation) between concrete slab and steel beam as well as steel connection and members (beams and column) requires the use of interface and/or non-linear spring elements, the constitutive non-linear laws of which can be defined in accordance with proposals available in literature [16,17].

4. Numerical analysis

The on-going numerical study was developed by means of the general purpose non-linear FE package ABAQUS [17], which is characterized by models as well as by material laws capable of modelling composite joints adequately. As model validation should be verified by the existing test data, in this initial phase attention was paid to the simulation of the nodal response of cruciform symmetrical specimens SJA10 and SJA14 (fig. 1a), which were tested under hogging moment [5].

The steel connection consists of a partial depth end plate welded to the beam and bolted to the

column (see fig. 1b) and the difference in the two specimens consists in the amount of the top longitudinal rebars: 8ø10 bars for SJA10 and 8ø14 bars for SJA14 specimen. The loads, monotonically increased up to collapse, were located at a slightly different distance from the column in order to preselect in which of the two joints collapse would occur.

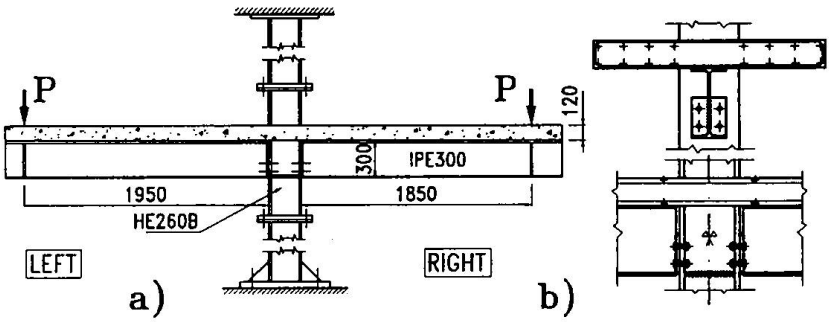

Fig. 1 The specimen (a) and the composite joint (b)

Attention was focused on both 2D and 3D models. Before 2D models were developed, a preliminary 3D elastic analysis on a quarter of the specimen, making use of the geometrical symmetry about both the web of steel beams and the column, as to reduce the problem size, permitted the effective width (fig. 2) for the definition of equivalent slab geometry to be assessed. Two-dimensional models (fig. 3) were built up with regard to complete or half specimen (FS and HS, respectively). Longitudinal rebars and bolts were modelled via truss elements and the action of the stud connectors, which provided full interaction in the considered specimens, was simulated via non-linear spring, the constitutive law of which was based on ref. [18]. Plane stress four node elements were used for the slab as well as for the other steel components (beam, column and connection plate). As to the material properties, an elastic-plastic law with strain hardening associated with the von Mises yield surface was selected for the steel components. For concrete, in addition to the concrete material model of ABAQUS (cma), which has been found in some cases not very efficient [11], a model based on von Mises yield criterion to deal with concrete cracking under tensile stresses (cmv) was also considered and the bond behaviour of rebars was simulated separately, in accordance with the results of ref. [19].

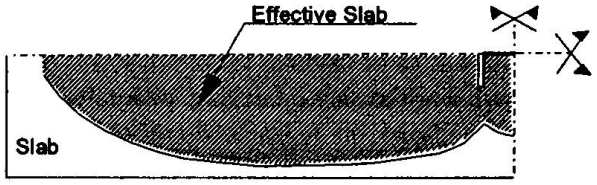

Fig. 2 Effective width of slab

As to 3D models, reference was made to a quarter of the specimen (3D HS in fig. 4). Eight node shell elements were selected for concrete slab, steel members and steel connection, while beam elements modelled the bolts. The same material law as in 2D simulations was considered for steel components while a smeared reinforcement was adopted for the concrete slab, for which the von Mises yielding criterion was adopted.

Both for 2D and 3D simulations, tension stiffening of concrete was considered in all the concrete models using the criterion proposed by Stevens [20], and unidirectional gap elements modelled separation/contact between steel connection and column flange as well as between concrete slab and top beam flange.

Figs. 5 and 6 present some of the numerical results, in terms of M-Φ curves, compared with the corresponding experimental responses. It appears that all the models can reproduce accurately the joint response in the elastic uncracked phases. With reference to 2D models, differences in the

other phases are due to the concrete material laws adopted (i.e., cma and cmv) as well as to the simulation of the explicit bond slippage of rebar in cmv model. The bond behaviour provides a more flexible response mainly in the elastic cracked branch.

A comparison between the 2D responses of half and full specimen, HS and FS, respectively, shows a limited influence of beam-to-column interaction, due to the presence of a modest unbalanced moment on the node. As to the 3D HS simulations, the degree of accuracy is slightly greater than the corresponding 2D HS ones mainly in the post-elastic phases, despite the 3D numerical curves are stiffer than the experimental M-Φ relationships.

Therefore, the predicted joint response reflects a trend generally in a good agreement with the test data and the cracking pattern is similar to the experimental one. The predicted collapse mode, due to plasticity of rebars, and consequently excessive joint deformation, as in the tests, was associate with ultimate moments in all the models very close to the actual joint moment capacity (differences lower than 5%).

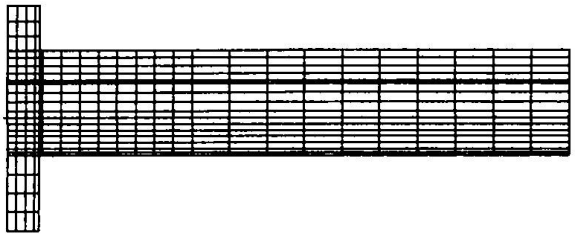

Fig. 3 Two-dimensional (2D) model

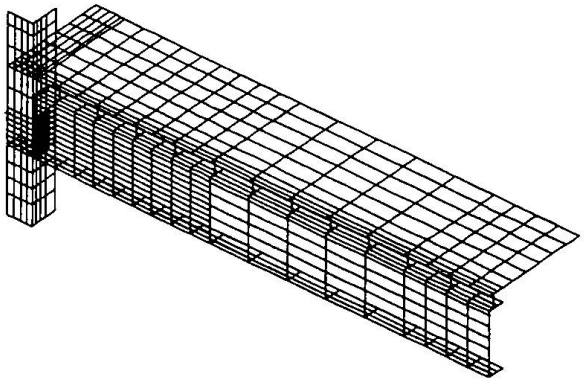

Fig. 4 Three-dimensional (3D) model

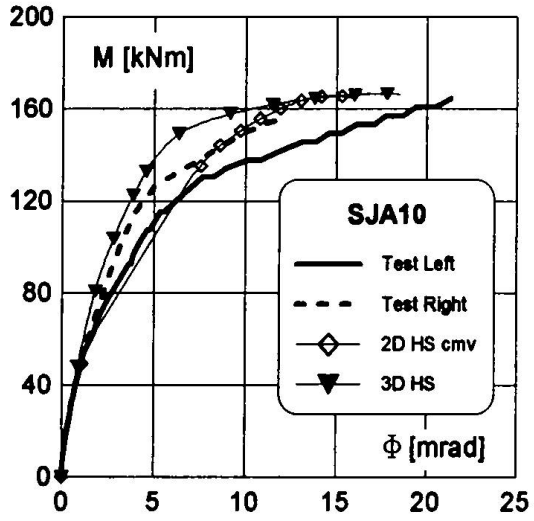

Fig. 5 Comparison of M-Φ curves for SJA10

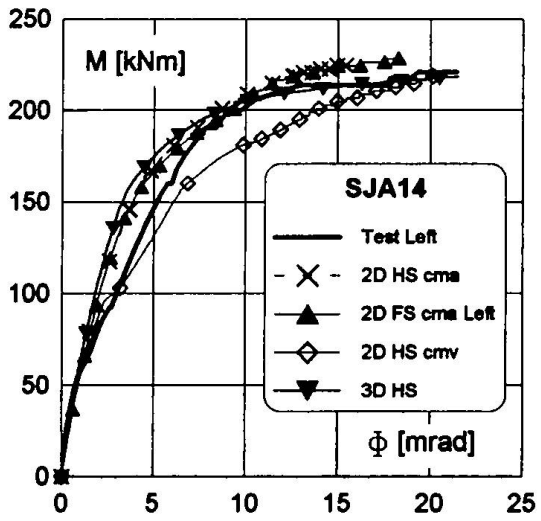

Fig. 6 Comparison of M-Φ curves for SJA14

5. Conclusions

This paper briefly reports an on-going study on the joint action simulation in steel-concrete composite systems. Key features of the nodal zone response are summarized and the general requirements of FE models, which can reproduce the main aspects of the physical behaviour of composite joints, are discussed.

Numerical simulations, carried out with reference to both 2D and 3D models, seem to be in a good correlation with test results and differences can be detected mainly in the post-uncracked phases of the M-Φ responses. The joint ultimate moment is assessed with a satisfactory degree of accuracy by all the models. Despite the 3D simulation is associated with better appraisal of the nodal behaviour, 2D model seems sufficiently accurate to estimate the joint response, if the key features of concrete slab are taken into account and modelled by means of suitable elements and material laws. As to future work, a complete analysis of the numerical results related to these as well as additional specimens would make possible an exhaustive understanding of the complex interactions between the components of the nodal zone.

Acknowledgements
The research project is supported by the National Research Council (C.N.R.) and by the Italian Ministry of the University and Scientific and Technological Research (M.U.R.S.T.).

References

[1] Zandonini R., 1989, "Semi-Rigid Composite Joints", in *'Structural Connection-Stability and Strength series: Vol. 8'*, Narayanan R. ed., Elsevier Applied Science ed., 63-120.
[2] Leon R.T. and Zandonini R., 1992, "Composite joints" in *'Constructional Steel Design: An International Guide'*, Harding J. et al. eds., Elsevier Applied Science, 1992.
[3] Zandonini R., Nethercot D.A., 1994, "Recent Studies on the Behaviour of Semi-Rigid Composite Connections", proc. of the ASCE Structural Conference, Atlanta, 1143-1148.
[4] Commission of the European Communities, 1994, "Eurocode 4-Design of Composite Steel and Concrete Composite Frames-Part 1.1 General Rules and Rules for Buildings".
[5] Benussi F., Puhali R., Zandonini R., 1989, "Semi-rigid Joints in Steel-Concrete Composite Frames", *Costruzioni Metalliche*, No. 5, 237-264.
[6] Puhali R., Smotlak I., Zandonini R., 1990, "Semi-rigid Composite Action: Experimental Analysis and a Suitable Model", *Journal of Constructional Steel Research*, Special Issue on Composite Construction, R. Zandonini ed., Vol. 15, Nos 1&2, 121-151.
[7] Benussi F, Bernuzzi C., Noè S, Zandonini R., 1996, "Experimental Analysis of Semi-Rigid Composite Frames", proc of the IABSE Colloquium: Semi-Rigid Structural Connection, Istanbul 1996, 105-113.
[8] Benussi F., Nethercot D.A., Zandonini R., 1995, "Experimental Behaviour of Semi-Rigid Connections in Frames", in *'Connections in Steel Structures III'*, R. Bjorhovde et al. eds., Elsevier Applied Science, 57-66.
[9] Nethercot D.A., Zandonini R., 1989, "Methods of Prediction of joint Behaviour: beam-to-column connections", in *'Structural Connection-Stability and Strength series: Vol. 8'*, R. Narayanan ed, Elsevier Appl. Science 23-62.
[10]Leon R., Lin J, 1986, "Towards the Development of an Analytical Model for Composite Semi-Rigid Connections", Report to AISC, Struct. Eng. Rep. No. 86-06, Univ. of Minnesota, Minneapolis, USA., p. 83.
[11]Ahmed B, Nethercot D.A., 1995, "Numerical modelling of Composite Flush End Plate Connections", *Steel Structures-Journal of Singapore Steel Society*, Vol. 6, No. 1, 87-102.
[12]Bursi O., Gramola G., 1997, "Smeared crack analysis of steel-concrete composite substructures", Stessa'97 Conference, Kyoto.
[13]Lee S.J. and Lu L.W., 1991, "Cyclic Load Analysis of Composite Connection Subassemblages", , in *'Connections in Steel Structures II'*, R. Bjorhovde et al. eds., American Institute of Steel Construction, 209-216.
[14]Kotsovos M.D., Pavlovic M.N., 1995, "Structural Concrete - Finite Element Analysis for Limit State Design', Thomas Teldfort Pub., p. 550.
[15]Lofti H.R., 1992, "Finite Element Analysis of Concrete and Masonry Structures", Ph.D. Thesis, University of Colorado, p. 148.
[16]Link R.A., Elwi A.E., 1995, "Composite Concrete-Steel Plate Walls: Analysis and Behaviour", *Journal of Structural Engineering*, Vol. 121, No. 2, 260-271.
[17]Hibbit, Karlsson & Sorensen Inc., 1996, "ABAQUS - User's manual, version 5.5", Vol. 1&2.
[18]Aribert J.M., 1988, "Critical Numerical Analysis of Methods Proposed by Eurocode for Dimensioning of Steel-Concrete Composite Beams with Partial Connection" (in France), *Construction Metallique*, Vol. 25(1)
[19]Eligehausen R., Popov E.P., Bertero V.V., 1983, "Local bond stress strain relationships of deformed bars under generalised excitation", Report N. UCB/EERC-83/23, University of California.
[20]Stevens, N.J., Uzumeri, S.M., Collins, M.P., and Will, G.T., 1991, "Constitutive Model for Reinforced Concrete Finite Element Analysis", *ACI Structural Journal*, V.88, No.1, 49-59.

Connection of Floor Systems to Columns - Conventional and Advanced

Ferdinand TSCHEMMERNEGG
Univ.-Prof.
University of Innsbruck
Innsbruck, Austria

Ferdinand Tschemmernegg, born 1939, got his civil engineering degree 1963 and his doctor degree 1968 from the Technical University Graz. After 17 years as a designer for bridges at different steel construction firms in Germany, he returned 1980 as Full Professor the University of Innsbruck, Austria.

Summary

Conventional and advanced joints, the development of modelling and the component method with assembly and transformation will be described. A summary of the work done in Innsbruck in this field complemented by application aids will be given.

1. Introduction

Connections between floor systems and columns are important elements in view of design and economy of buildings.

Steel beam-to-column connections in building frames are called **conventional connections**. The floor slabs, which are or are not connected to the lower floor beams, were not integrated into the connection. They were even clearly separated from the column by a gap. This is uneconomic but there was no research available for design of the interaction between the floor slabs and the columns.

In **advanced composite connections** the floor slabs connected to the floor beams below are included in the connection to the column. In a further step the floor beams themselves are already integrated into the floor slabs (slim floors) and connected to the column. This is much more economic because the steel structure can be erected in a very simple way with steel beam-to-column connections and after concreting of the floor slabs the connections automatically get high stiffness, strength and rotation capacity.

The connection between the floor system and the column is only one part of a **joint**. The second one is the part of the column within the depth of the floor, see Fig.1,2.
The basic idea of the research was to study the non-linear member force-deformation behaviour (M-Φ) of the joint as a separate element with finite size.

2. Non-linear Behaviour of a Joint

2.1 Kinds of joints

Fig.1 shows some examples of conventional and advanced joints.

2.2 Joint Modelling

In Fig.2 the development of joint modelling is shown. Conventional global analysis assumed rigid joints of infinite small size. But as any real joint has a finite size deformations occur under relevant member forces. So in this traditional view the beam and column stubs (bj, hj acc. Fig.2,3) can be understood as a part of the deformation of the real joint.
The first step of improvement was to regard the joint as a separate element of finite size. In [1] the idea of the so-called component model was published for the first time.
The second step was to describe the force-deformation behaviour of all individual components by non-linear translational springs [1,2,3].

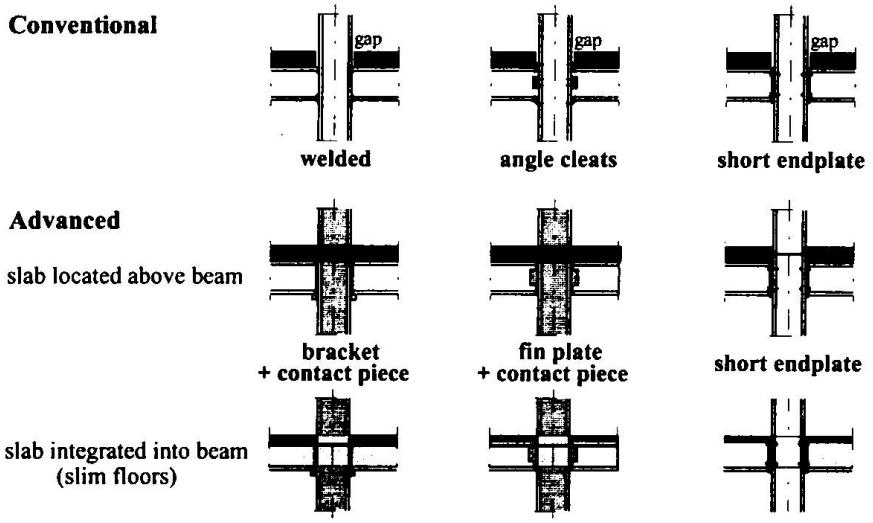

Fig. 1 Kinds of joints

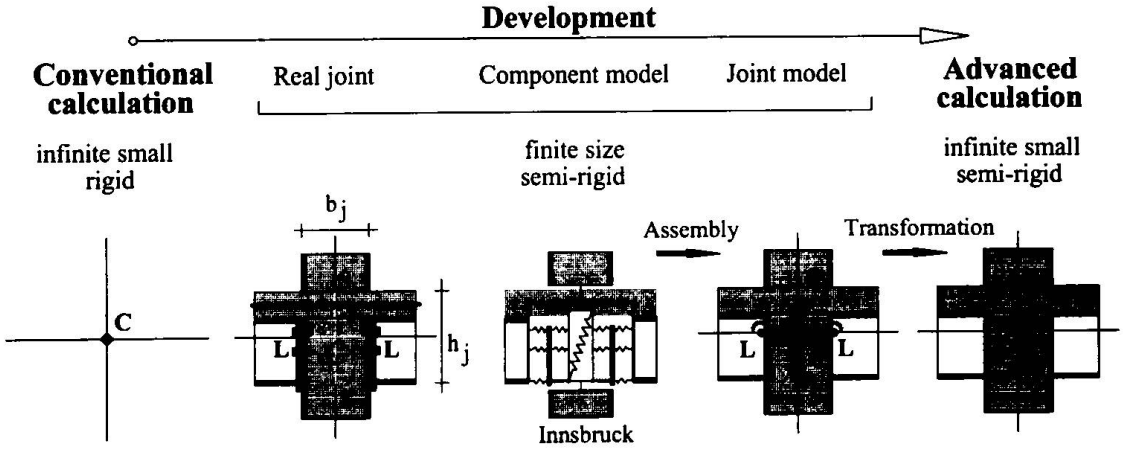

Fig. 2 Joint modelling

In the third step the translational springs are assembled to rotational springs in L and S. The rotational spring in L includes the loadintroduction into the column and the deformation of the connection. The rotational spring S represents the shear deformation of the part of the column within the depth of the floor. In the global analysis the parts of beams and columns within the region of the joint are set infinite rigid. All deformations of the joint are represented by the rotational springs in L and S forming the Innsbruck Joint Model.
For simplification in the fourth step the rotational springs in L and S are transformed back to the centre C.

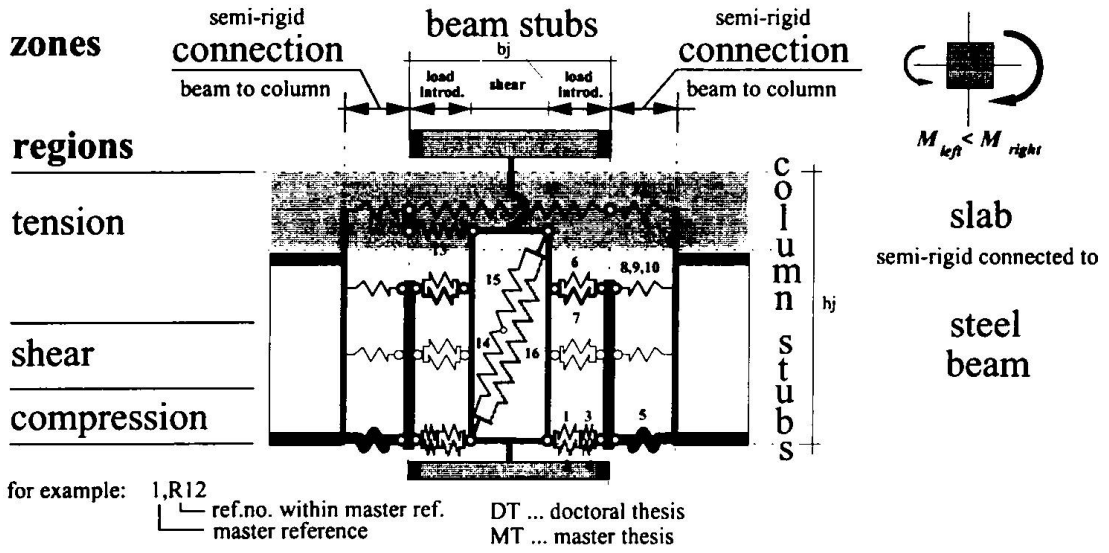

No.	component	zone	region	column section I DT	I MT	□O DT	□O MT
1	interior steel web panel	stubs	compression	2,R3 3,R4	3,R11 3,R12 3,R13 3,R15 3,R16	8 9	10 11 12 13 14
2	**concrete encasement**	stubs	compression	3,R4	3,R17 3,R18	8 9	10, 11, 12, 13, 14, 15
3	exterior steel web panel (column flange+local effects)	stubs	compression	3,R4	3,R13 3,R15	8 9	10, 11, 12, 13, 14
4	**effect of concrete encasement on exterior spring**	stubs	compression	3,R4		8 9	10, 11, 12, 13, 14, 15
5	beam flange (local effects), contact plate, end plate	*connection*	compression	3,R4		8 9	
6	steel web panel incl. part of flange, fillet radius	stubs	*tension*				
7	stiffener in tension	stubs	*tension*				
8	column flange in bending (stiffened)	*connection*	*tension*	2,R5			
9	end plate in bending , beam web in tension	*connection*	*tension*	2,R5			
10	bolts in tension	*connection*	*tension*	2,R5			
11	**reinforcement (within panel) in tension**	*stubs / conn.*	*tension*	3,R5		3,R5	
12	**slip of composite beam (due to incomplete interaction)**	*stubs / conn.*	*tension*	3,R6			
13	**redirection of unbalanced forces**	*stubs / conn.*	*tension*	3,R5		3,R5	
14	steel web panel in shear	stubs	*shear*	2,R4 3,R3	3,R9 3,R14	8 9	10, 11, 12, 16
15	steel web panel in bending	stubs	*shear*	3,R3	3,R9	8 9	10, 11, 12, 16
16	**concrete encasement in shear**	stubs	*shear*	3,R3	3,R9	8 9	10, 11, 12, 16

Fig. 3 Innsbruck component model

2.3 Component Model

Fig.3 shows the Innsbruck component model considering all relevant components of conventional and advanced joints. In numerous tests the non-linear force-deformation behaviour was studied in so-called component tests. Fig.3 gives an overview of all component tests and corresponding literature acquired in Innsbruck. It has been proved on tests on full-scale joints that the component model is adequate [3,R3,4,5]. The test results were brought into the international databank SERICON [4,5] and were used for standardisation in [6,7].

2.4 Assembly

In Fig.4 the assembly procedure is shown. Out of the tests models for each individual component were developed as translational springs, describing the stiffness, strength and ductility analytically. The individual springs then are joined together in series or parallel forming spring groups. These spring groups are finally assembled to rotational springs in L (loadintroduction and connection) and S (shear).

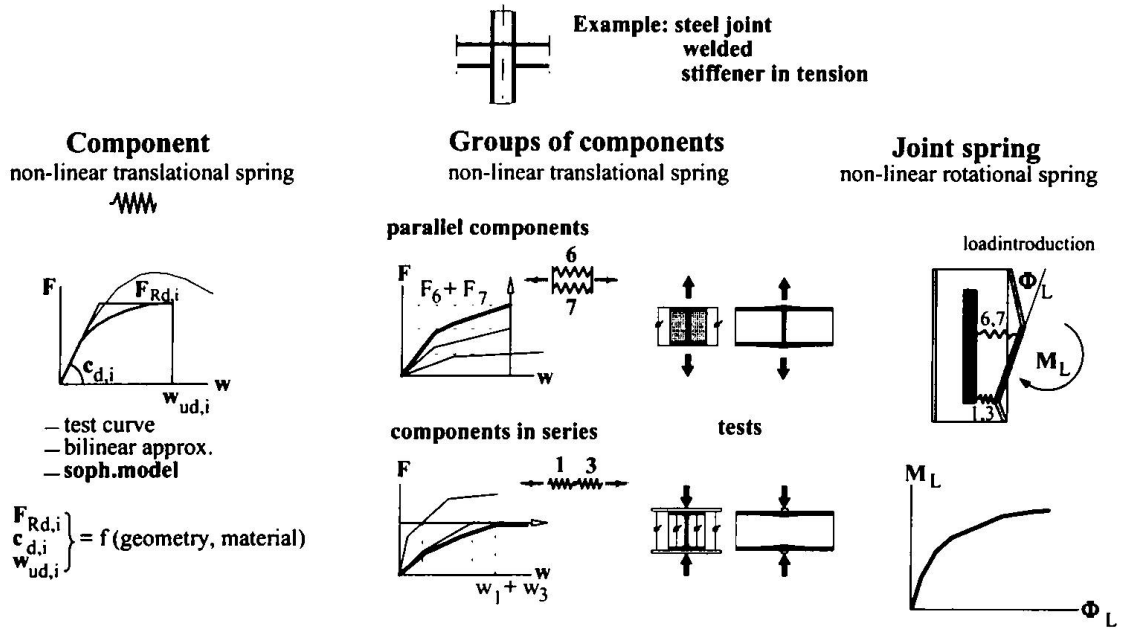

Fig. 4 Assembly

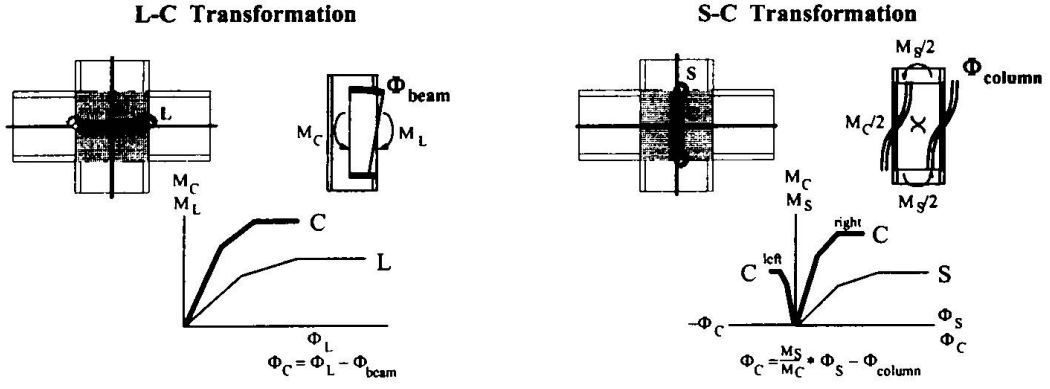

Fig. 5 Transformation

2.5 Transformation

Transforming the rotational springs in L and S to C it must be considered, that the beam and column stubs in the region of the joint get deformations from the global analysis, Fig.5. So these deformations, which mainly depend on the joint itself, have to be subtracted from the deformations of the joint not to have this influence twice in the global analysis. It should also be noted especially for big joints in relation to the structure that the moment increases from S and L to C depending on the global analysis.

3. Application aids

The author realises that until now the practical application for all this new knowledge is rare. In Austria only one building was designed making use of all composite elements as slabs, beams, columns and joints [17]. The reason is, that practical engineers are not trained to use non-linear calculations and support like adequate tables, handbooks and software is missing.
A general problem today is the technology transfer because of missing money. The money available is just enough for the basic research but twice as much money would be necessary for the work-out of practical application rules and tables together with partners from the industry.
In Innsbruck success has already been achieved with the following efforts:

3.1 Tables for joint calculation

In two master thesis tables for short endplate steel joints and corresponding tables for composite joints were developed. The tables dealing with steel joints are useful for the calculation of erection, whereas those for the composite joints help for the calculation of the final composite structure [18,19].

3.2 Software for joint calculation

On the basis of the Innsbruck model the Module Bank System [20] determines the M-Φ-curves of steel and composite joints. As it is an open system it can continuously be adopted to the latest knowledge, especially considering the assembly and transformation as well as new components like loadintroduction and shear in hollow steel and composite column sections.

3.3 Software for frame calculation

With the software [21,22] sway frames including the non-linear behaviour of the joints can be analysed.
An instrument for the calculation of continuous beams considering the material non-linearities, the tension stiffening effect, the non-linear interaction between the beam and the slab and the non-linear behaviour of the joints will be provided in [23].

4. Conclusion and Acknowledgement

Advanced composite joints have the advantage that the slab of the floor is integrated into the joint. This is especially important for the execution of the building in view of costs. Out of the component method a lot of new joint configurations with simple erection methods can be derived in the future. The theoretical basis is well advanced, so the practical application should be forced.

The author thanks all the assistants and students for their important contribution to this research, the Austrian Research Foundation for the industries (FFF Vienna) and the steel and concrete industry for the financial support of the whole project.

5. References

[1] ÖSTV, SZS: Rahmentragwerke in Stahl unter besonderer Berücksichtigung der steifenlosen Bauweise, Österreichischer Stahlbauverband, Schweizerische Zentralstelle für Stahlbau, Wien/Zürich, 1987.

[2] TSCHEMMERNEGG F., et al: Zur Nachgiebigkeit von Rahmenknoten, Stahlbau 56, p.299-306, Stahlbau 58, p.45-52, Berlin 1987, 1989.

[3] TSCHEMMERNEGG F., et al: Zur Nachgiebigkeit von Verbundknoten, Stahlbau 63, p.380-388, Stahlbau 64, p.16-24, Berlin 1994, 1995.

[4] HUTER M.: Internationale Versuchsdatenbank für Stahl- und Verbundknoten, Doctoral thesis, Innsbruck, 1997.

[5] WEYNAND K.: SERICON - Databank on joints in building frames, COST-C1 Workshop, p.465, Strasbourg, 1992.

[6] ENV 1993-1-1, pr A2: Design of steel structures, General rules and rules for buildings, Revised Annex J: Joints in building frames, 1994.

[7] TSCHEMMERNEGG F., HUBER G.: Technical papers T1 to T10. Calibration work within COST-C1/ECCS TC11 Drafting Group for Composite Connections for ENV1994-1-1, Annex J, Innsbruck, 1995-1997. WWW-access: http://info.uibk.ac.at/c/c8/c809/res/cost/wg2/drgroup password for downloading postscript-files = modelibk

[8] FINK A.: Das Momentenrotationsverhalten von Verbundknoten mit Verbundstützen aus Rechteckshohlprofilen, Doctoral thesis, Innsbruck, in work.

[9] MÜLLER G.: Das Momentenrotationsverhalten von Verbundknoten mit Verbundstützen aus Rohrprofilen, Doctoral thesis, Innsbruck, in work.

[10] STEINER M.: Teiluntersuchungen zu Verbundknoten mit Hohlprofilstützen - Großversuche und Komponentenversuche, Master thesis, Innsbruck, in work.

[11] WINKLER B.J.: Versuche zur Ermittlung des Schub- und Krafteinleitungsverhaltens von Rechteckhohlprofilen mit und ohne Betonfüllung, Master thesis, Innsbruck, 1995.

[12] ZANGERL O.: Versuche zur Ermittlung des Schub- und Krafteinleitungsverhaltens von Rohrprofilen mit und ohne Betonfüllung, Master thesis, Innsbruck, 1995.

[13] AIGNER M.: Detailuntersuchungen für Anschlußprobleme von Flachdecken an runde Stahlprofile und Verbundprofile , Master thesis, Innsbruck, 1996.

[14] AMPFERER G.: Detailuntersuchungen für Anschlußprobleme von Flachdecken an rechteckige Stahlstützen bzw. Verbundstützen , Master thesis, Innsbruck, 1996.

[15] DORNETSHUBER J.: Zur Krafteinleitung in Verbundknoten mit Rohrprofilen, Master thesis, Innsbruck, 1990.

[16] STOIBERER H.: Zur Querkraftdeformation von Verbundknoten mit Rohrprofilen, Master thesis, Innsbruck, 1990.

[17] TSCHEMMERNEGG F., et al: Servicestation in Mischbauweise - Bemessung nach ENV 1993-1, 1994-1, Stahlbau 65, p.180-187, Berlin, 1996.

[18] HASLRIEDER K.: Bemessungsbehelfe für Stahlknoten mit Stirnplattenanschlüssen nach ENV 1993-1-1, prA2, Revised Annex J, Master thesis, Innsbruck, 1996.

[19] SEEBER K.: Bemessungsbehelfe für Verbundknoten mit Stirnplattenanschlüssen nach ENV 1994-1-1, draft Annex J, Master thesis, Innsbruck, 1997.

[20] SCHAUR B.C.: Entwicklung einer Modulbank für Stahl- und Verbundknoten, Doctoral thesis, Innsbruck, 1995.

[21] LENER G.: Berechnung räumlicher Stahlrahmen mit nichtlinearem Knotenverhalten unter Berücksichtigung der Normalkraftinteraktion, Doctoral thesis, 1988.

[22] LENER G.: Programmsystem Plan V3.1, Computer Manual, 1988.

[23] HUBER G.: Non-linear calculations of composite floors considering the interaction with semi-rigid joints, Doctoral thesis, in work.

The Use of Composite Connections in Practice

Graham COUCHMAN
Principal Engineer
SCI
Ascot, UK

Graham Couchman was educated at Cambridge University before spending five years working for Taylor Woodrow construction. He obtained his PhD. in 1994 from the Swiss Federal Institute of Technology in Lausanne. He is currently producing several design guides dealing with the interaction of frame and connection behaviour.

Mark LAWSON
Senior Manager, Structures
SCI
Ascot, UK

Mark Lawson obtained his PhD. from the University of Salford and worked for 4 years with Ove Arup and Partners. He later became Research Manager at CIRIA in London, and then Senior Manager, Structures at The Steel Construction Institute. His specialisations are composite construction, light steel construction and fire engineering.

Summary

For any new design approach to be adopted by practising engineers, genuine benefits must be attainable without a disproportionate increase in design effort. Making use of semi-continuity between the members of a frame offers the potential for significant benefits. A design guide is currently being developed which demonstrates how these benefits can be realised in braced composite frames. The manual provides both frame and connection design procedures, and includes tabulated information to reduce design effort.

1 Introduction

Semi-continuity between frame members can be used to reduce the overall cost of a steel or composite frame. Beams can be shallower or lighter than in "simple construction", and connections require considerably less fabrication effort than those in continuous frames. Connection performance has a major influence on frame behaviour.

It is essential that in developing frame analysis and design methods, consideration is given to both simplicity and the connection characteristics that are required in order to use the method. The three principal connection characteristics are rigidity, strength and ductility (or rotation capacity). Plastic analysis at the ultimate limit state (ULS) benefits from being simple. Its use requires the connection strength (moment resistance) to be predictable with reasonable accuracy. Connection ductility is also essential. Models exist for calculating strength, whilst adequate ductility can be proven by testing when standard details are used, or by using appropriate detailing rules. In contrast, elastic analysis relies on an ability to quantify connection rigidity. Current methods are labourious, and do not allow this quantification with sufficient accuracy for ULS calculations. However, more approximate predictions of rigidity are acceptable for calculating frame performance at the serviceability limit state (SLS).

A *Composite Connections Manual* is currently being produced by the Steel Construction Institute (in conjunction with academics, consulting engineers and fabricators), that considers both composite connection and braced frame design. The composite connections are based on standard details which achieve continuity through both the steel connection itself, and the

tensile reinforcement in the slab. This paper presents some of the principal sections in the manual.

2 Standard Connection Manuals

The SCI/BCSA Connections Group was established to develop industry standards for structural steelwork connections in the UK. The benefits of standard connections include;

- connection characteristics can be accurately determined by testing or semi-empirical methods calibrated against tests on similar details,
- reduced disagreements between designers (frame members are traditionally designed by a consulting engineer, and connections by a fabricator),
- the development of software is encouraged (using agreed procedures),
- standard connection capacities can be tabulated to reduce design effort,
- a manufacturing approach to connections is promoted (using rationalised components),
- reduced uncertainty at the tendering stage,
- reduced errors (when bolt sizes and grades are rationalised),
- avoidance of expensive, difficult to erect connection details.

The group have already produced three manuals dealing with steelwork connections. These will be complemented by the current work on a manual for composite connections.

3 Composite Connections Manual

3.1 Potential Benefits

Any new design method which involves even minor changes to existing practice will only be adopted if genuine and significant benefits can be demonstrated.

A study undertaken by the SCI has shown that it is possible to reduce the depth or weight of an individual beam by up to 25%. Depth savings may be particularly important, allowing easier integration of services, reduced cladding costs etc. However, to achieve genuine benefits, savings must be possible for a substantial number of the beams in a given frame. For example, if the designer is aiming for depth savings, these may need to apply to all the beams in a floor if cladding costs are to be reduced. Depth savings in certain zones may be sufficient to facilitate service integration. The choice of frame layout has a major influence on the overall benefits that can be achieved, as explained below.

3.2 Frame Layout

The size of a beam in a composite frame is generally governed by one of two conditions;

- the moment resistance of the composite beam at the ULS,
- the total deflection of the beam at the SLS, the greater part of this deflection being due to the weight of the slab applied to the steel beam during (unpropped) construction.

Table 1, taken from the manual, indicates which condition governs for a range of loading

types and steel grades. The table is applicable for spans up to 12m. A question mark (?) indicates that either condition might govern. The beam span to depth ratio is also a useful indicator of the relative importance of ULS and SLS conditions. Limits are suggested in the manual for different scenarios. If the benefits of using semi-continuity are to be realised, connections to beams which are governed by composite moment resistance at the ULS should be detailed to provide strength. Connections to beams which are governed by SLS deflections should be detailed to provide rigidity. Rigidity in the bare steel state is essential to reduce the construction stage component of the total deflection. Certain other recommendations should also be considered when choosing the frame layout:

Loading	Steel Grade	Critical Condition	
		SLS	ULS
Distributed	S355	x	
	S275	?	?
Central point	S355		x
	S275		x
Points at third span	S355	?	?
	S275		x
Multiple points	S355	x	
	S275	?	?

Table 1: Conditions which govern beam design

- Orthogonal connections to a column should not both be composite. This restriction is imposed to prevent over congestion of reinforcement.
- Connections to perimeter columns should not rely on composite action, since anchorage of reinforcement is difficult to achieve at the slab edge. Connections to perimeter columns are therefore relatively weak, and excessive unbalanced moments are not introduced into the columns. When moments are large, local strengthening, or an increase in column section size, may be necessary.

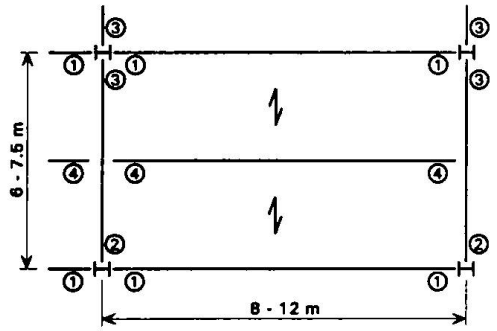

Connection Type	Principal Characteristics
1	Rigid, Steel
2	Pinned, Steel
3	Strong, Composite
4	Pinned, Steel

Figure 1: Typical floor beam layout to achieve beams of similar depth

Possible framing arrangements which capitalise on these principles, and corresponding connection details, are suggested in the manual. One possible framing arrangement is reproduced in Figure 1. Note that for maximum benefit the connection Type 4 in Figure 1 would need to be rigid in the bare steel state. Unfortunately, rigidity is difficult to achieve for a beam to beam steel connection, making the use of a nominally pinned connection unavoidable in most such situations.

3.3 Frame Design

3.3.1. Plastic hinge analysis at ULS

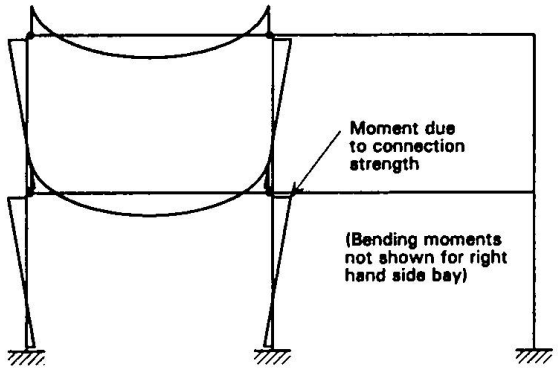

Figure 2: Moment distribution at the ULS

Beam design is based on the assumption that plastic hinges form in the connections. The resulting negative (hogging) moments at the beam ends allow the required beam plastic moment resistance to be reduced. This is shown schematically in Figure 2. The assumption that plastic hinges form is only valid when the connections possess sufficient ductility, which has been shown by testing for the standard details.

Internal columns are designed for axial load only, caused by imposed load applied to all the beams. Pattern loading cases with reduced axial load combined with moment applied to the column have been shown to be less critical by testing and finite element analyses [CIMsteel *Semi-continuous braced frames*]. This means that column design is no more complicated than that for columns in "simple" frames according to BS 5950. Perimeter columns are designed for axial load combined with an unbalanced moment equal to the connection capacity.

3.3.2. Elastic analysis at SLS

Connection rigidity reduces beam deflections significantly. By using standard connection details, rigidity can be quantified with acceptable accuracy for deflection calculations, based on test results.

The SLS procedures given in the manual build on previous work by the first author [CIMsteel *Semi-continuous braced frames*], providing simple formulae to conservatively calculate deflections. For example, the deflection of an internal beam subject to distributed loading is given by $\delta = 3/384\ (wl^4 / EI)$. (This equation is based on the rigidity of the standard connections, and may be subject to minor adjustment as development work on the manual progresses.) Formulae are given for various load arrangements and end conditions. For less common situations, or when more accuracy is needed to reduce calculated values, a full procedure taking into account specific member and connection rigidities is given in an appendix.

3.4 Outline Procedure for Beam to Internal Column Connections

One of the standard connection types featured in the manual is a composite connection framing into the column flange. Such a connection could be used to reduce the moment resistance required from a beam at the ULS, and offers reasonable rigidity in both the bare steel and composite states.

The outline procedure for calculating connection moment and shear resistances is described in the manual. Components which have a significant influence are the;

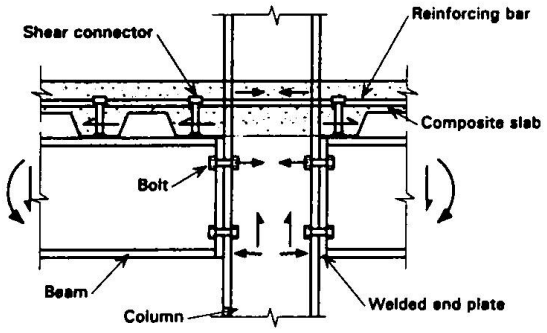

Figure 3: Connection components

- tensile resistance of the reinforcement,
- tensile resistance of the upper bolts,
- compression resistance of the beam lower flange,
- compression resistance of the column (considering buckling and bearing),
- longitudinal shear transfer between the beam and slab,
- shear capacity of the bolts.

These are shown in Figure 3.

In addition to resistance, sufficient ductility is essential if the frame design procedures described in the manual (see Section 3.3) are to be adopted. Detailing rules to ensure ductility are described in the manual, and the standard connections have been shown by testing to be satisfactory. A minimum percentage reinforcement (1% of the slab cross-sectional area) is necessary to give sufficient ductility.

3.5 Step-by-Step Connection Design Procedure

Step-by-step design procedures for the principal connection types are given in the manual, and are illustrated by worked examples. These procedures could be used to design a connection by hand, but are more likely to be used to write software. As with previous connection manuals, a software producer is included in the task group responsible for draughting. The benefits of this relationship include;

- the logic of procedures is verified as they are translated into coding and tested,
- commercial software to simplify the connection design process will be available upon publication of the manual.

3.6 Design Tables

Two types of table are included in the manual; tables which give moment and shear resistance for a range of standard connections, and tables which give the physical details of these connections.

The resistance tables will simplify the work of designers by eliminating extensive calculations when standard details are adopted. In choosing a standard detail, the designer will also be assured that the connection;

- is ductile (has sufficient rotation capacity),
- has sufficient rigidity,
- can be fabricated economically (since it is based on fabricators' recommendations).

An extract from a typical table showing the moment resistance of a range of composite "major axis" connections is given in Table 2. Moment resistance is expressed as a function of the

composite beam resistance in sagging. It can be seen that the connection moment resistance increases as reinforcement is added. However, the tensile force in the bars must be balanced by compression in the column, and if an excessive amount of reinforcement is added the column will require local strengthening. Supplementary tables in the manual therefore indicate the maximum percentage of reinforcement which can be used with different column sizes before local strengthening is required.

Steel Beam Section	Percentage of slab reinforcement				
	0.5%	1.0%	1.5%	2.0%	2.5%
533x210x122	0.09	0.19	0.28	0.38	0.47
533x210x109	0.10	0.21	0.31	0.41	0.52
533x210x101	0.11	0.22	0.33	0.44	0.55

Table 2: Connection moment resistance expressed as a proportion of the composite beam positive (sagging) moment resistance, for S355 beams.

Considering the physical details of the connections, it was decided from the outset that only one solution would be given to a particular problem. One of the reasons for this approach is to avoid complications when the frame members and connections are designed by different parties. It was felt that if alternative (e.g. cleated, fin plate or end plate) details were provided there would always be cases when a consultant specified one type of detail, and the fabricator wished to use another. Because frame behaviour is inextricably linked to connection behaviour this would necessitate a review of the member design. If only one option is available there can be no arguments! Perhaps a more legitimate reason is that steel end plate details are the most suitable for use in composite connections, because they provide a direct load path for compression from the beam bottom flange to the column, and have sufficient rigidity to facilitate erection.

The over-riding philosophy for connection detailing is one of avoiding complexity; local column strengthening is avoided if possible, to keep fabrication and therefore costs down to a minimum. If a chosen detail requires local strengthening, this can be avoided either by choosing an alternative detail or by increasing the column section size.

4 Conclusions

Two criteria must be satisfied for any new idea to be adopted by practising engineers;

- genuine benefits are achievable,
- design methods are simple, and appropriate aids (tables and software) are available.

The manual currently being produced demonstrates how the benefits of semi-continuous composite frames can be realised, and presents details and procedures which are based on the knowledge and experience of a broad cross section of practitioners. It includes design tables which simplify the work of both the frame designer and the fabricator. Software is being developed in parallel with the manual.

A New Steel-Concrete Composite Building with Double-floor System

Koji YOSHIMURA
Professor
Oita University
Oita, Japan

Ikuo IIDA
President
IIDA Design and Planing Office
Oita, Japan

Kenji KIKUCHI
Associate Professor
Oita University
Oita, Japan

Koji OKITA
President
Renace Institute
Oita, Japan

Summary

In order to create a better residential environment in human life, it is necessary to offer a higher quality of apartment building which has sufficient storage spaces and adequate sound transmission insulation between adjacent two stories. Herein, a new steel reinforced concrete (SRC) apartment building having double-floor system is proposed to satisfy these requirements within a limited floor space, and SRC inverted T-shape and L-shape specimens are tested to develop a better reinforcing method within slab-to-beam connections of the double floor system.

1. Introduction

According to the latest investigation report by the Ministry of Construction of Japanese Government, more than 50 percent of one-hundred thousand householders jointing this investigation have their dissatisfactions on narrow storage spaces and noisy sound transmission from the upper-story residents [1]. In order to solve these problems within a limited floor-space area and to offer a higher quality for dwelling environment in multi-story residential buildings, a new type of apartment building having double-floor system was already proposed by authors, and the first reinforced concrete (R/C) building with seven stories was built in 1994 in Oita City, Japan [2,3].

Fig. 1 shows a schematic illustration of the double-floor slab system adopted in a thirteen-story steel reinforced concrete (SRC) apartment building which was completed in 1996 in Fukuoka City, Japan. This building has nearly the same floor area with ordinary apartment buildings widely constructed in Japan, but the only one difference in structural system is that this has a double-floor slab system to insulate the sound transmission from upper-story residents and to provide satisfactory storage spaces between top and bottom floor slabs. Each of the top floor of this double-floor system is a lumber decking which is composed of plywoods and light-gage steel sub-beams without any intermediate supports. On the contrary, each bottom floor is an R/C suspended slab which has an inverted T-shape or L-shape cross-section at the R/C-slab to SRC-beam connections. In this type of inverted T-shape slab-to-beam connections, however, systematic experimental study about the effect of reinforcing details on its structural behavior has not been conducted sufficiently.

Main objective of the present study is to examine the structural behavior of inverted T-shape and L-shape suspended slabs experimentally and to propose a better reinforcing method for strength and ductility of this type of suspended slab system.

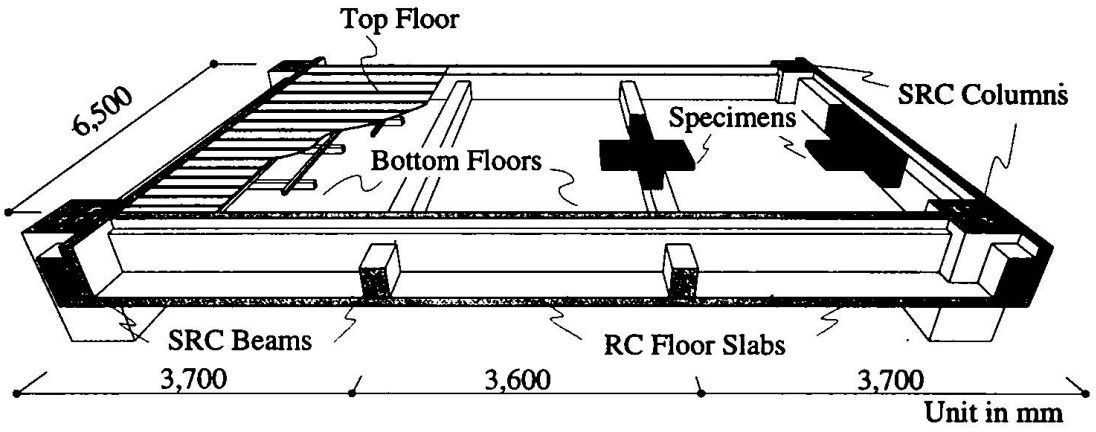

Fig. 1 Double-floor slab system

In the present experimental study, five different full-scale specimens with inverted T-shape and L-shape slabs were tested under monotonic vertical loads and test results were compared with those obtained from the ordinary T-shape specimen.

2. Test Specimens

A total of six full-scale specimens with different slab-to-beam connection details were designed and constructed. Five specimens have suspended slabs with inverted T-shape and L-shape cross-sections, and only one specimen has an ordinary T-shape cross-section. Each specimen is composed of one SRC beam element and one or two R/C slab elements connected each other at the top of the beam for the T-shape specimen and the bottom of the beam for the inverted T-shape and L-shape specimens, respectively. Fig. 2 shows size and shape of the inverted T-shape and L-shape specimens, which correspond to slab-beam segments as shown in Fig. 1.

Reinforcing details for all the specimens are listed in Table 1 together with the material properties of concrete and Re-bars, and the details of all the specimens are respectively shown in Fig. 3. Specimen (SRC-OT) in Fig. 3 is a model of ordinary T-shape beam-slab subassemblage in case

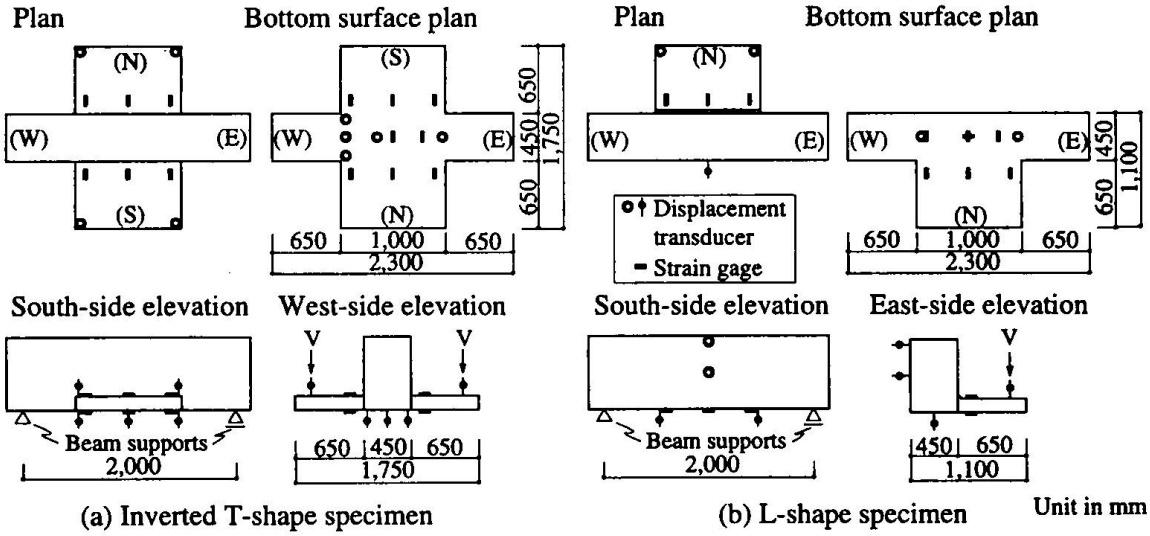

Fig. 2 Size and shape of inverted T-shape and L-shape specimens

Table 1 List of specimens

Specimens	Reinforcement			Compressive Strengths of Concrete [kgf/cm²]	Yield Strengths of Slab Re-bars	
	Slab Re-bars		Slab-to-beam Connection		Bar Size	
	Top Bars	Bottom Bars	Diagonal Re-bars		D13(#4) [kgf/cm²]	D10(#3) [kgf/cm²]
SRC-OT	D13(#4) D10(#3) Alternate @200	D10(#3) @400	None	275	3760	3710
SRC-IT				252		
SRC-ITH1			D13(#4) @200	277		
SRC-ITH2				211		
SRC-LH				251		
SRC-LHS				246		

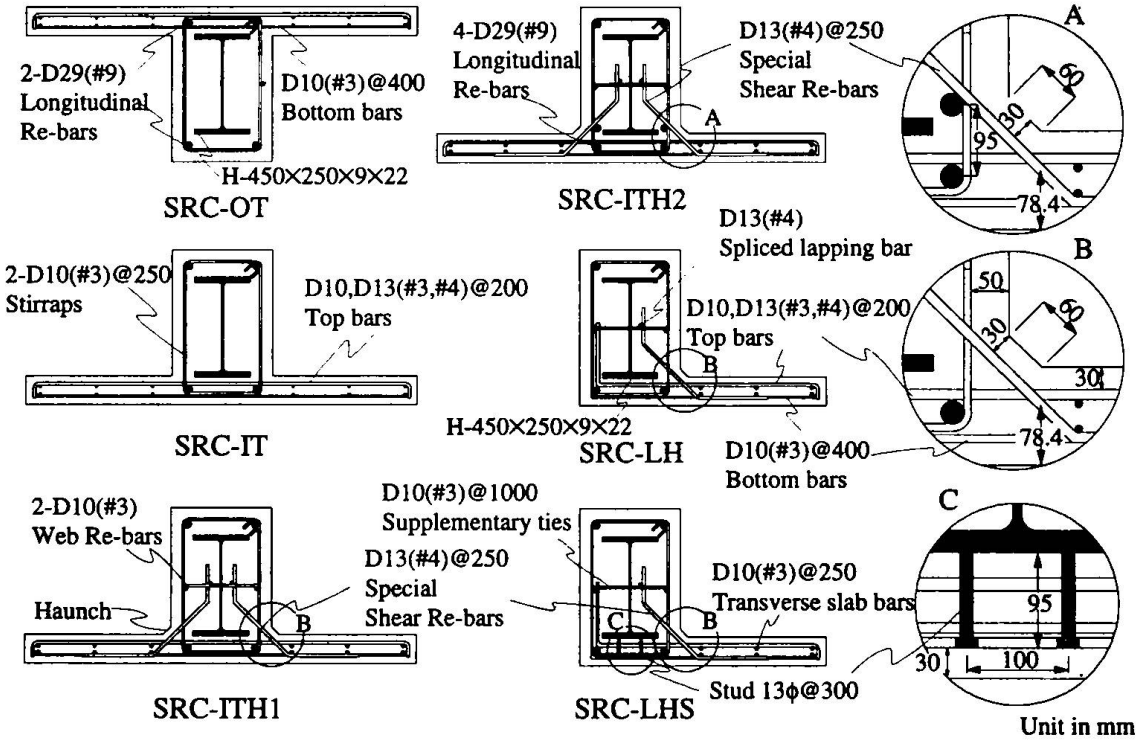

Fig. 3 Reinforcing details in slab-to-beam connection

when floor slabs of the similar building shown in Fig. 1 are designed by using an ordinary T-shape slab system, where required amount of reinforcement and connection details are designed in accordance with the current structural design standard in Japan [4].

Other three specimens in Fig. 3 are inverted T-shape specimens with different reinforcing details. Slab-to-beam connection of Specimen (SRC-IT) has the same reinforcing details with Specimen (SRC-OT) except that the slabs are located at the bottom of the beam. In addition to this slab-to-beam connection detail, special diagonal shear reinforcements and haunch are provided in Specimens (SRC-ITH1) and (SRC-ITH2) as shown in Fig. 3. Only one difference between reinforcing details of Specimens (SRC-ITH1) and (SRC-ITH2) is the total number of longitudinal Re-bars provided at the bottom of each beam. Specimen (SRC-ITH2) was adopted to investigate

the effect of congestion of reinforcement on the structural behavior of slab-to-beam connection.

In Specimens (SRC-LH) and (SRC-LHS), only one slab is provided along the bottom of spandrel beam. Slab-to-beam connection of Specimen (SRC-LH) has the corresponding reinforcing details to those of Specimen (SRC-ITH1) in Fig. 2. Specimen (SRC-LHS) has the same reinforcing details with Specimen (SRC-LH) except that some studs are welded at the bottom of wide flange surface in the steel H-shape beam.

3. Test Setups

Experiments for the ordinary T-shape, inverted T-shape and L-shape specimens were respectively conducted by using the test setups shown in Figs. 4(a), (b) and (c). All the test specimens were simply supported at both ends of their beam. Vertical load to the slab-end, V, was applied as a concentrated line load, the loading point of which was 50 cm from the beam face as shown in Figs. 4(a), (b) and (c). Application point of this vertical loading was determined so as to be equivalent when the same slabs were subjected to design dead plus live loads specified in the Building Code and Standard of Japan [4,5].

"Displacement Controller (or Pantograph)" shown in Figs. 4(a) and (b) was designed and installed in order that both of the vertical displacement at the North and South loading points can be kept equal all through the experiment. "Reaction Beam" shown in Fig. 4(c) was to prevent the rotational movement of the beam.

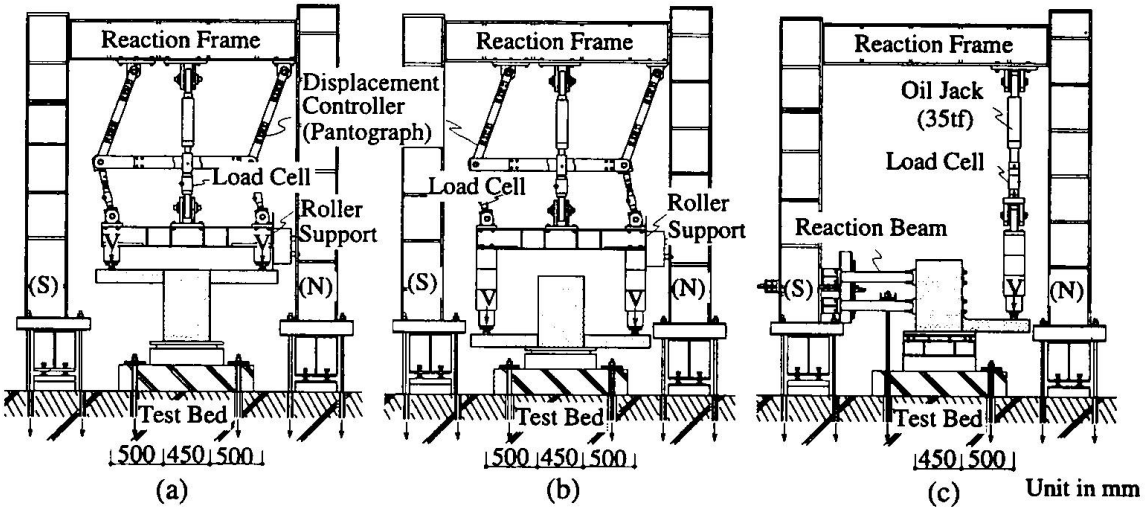

Fig. 4 Test setups for (a) ordinary T-shape, (b) inverted T-shape and (c) L-shape specimens

4. Test Results and Discussions

Fig. 5 represents the applied vertical load (V) versus corresponding vertical displacement relations for all the specimens. In the figure, bending moment (M) applied to each of the slab-end is also presented. For the T-shape and inverted T-shape specimens, these values of V and M are the averages of two measurements, and δ is the average of four measurements at the North and South slabs. Along each curve of the V-δ relations in Fig. 5, information obtained from the strain-gage measurements or visual observation is also given by using the open circle, open square and solid triangle, which mean the initiations of tension-yielding in top and bottom bars for slab main reinforcement and crushing of compression-concrete at the slab-to-beam connections, respectively. Also in this figure, the allowable strengths for long-term loading [4] and the ultimate strengths

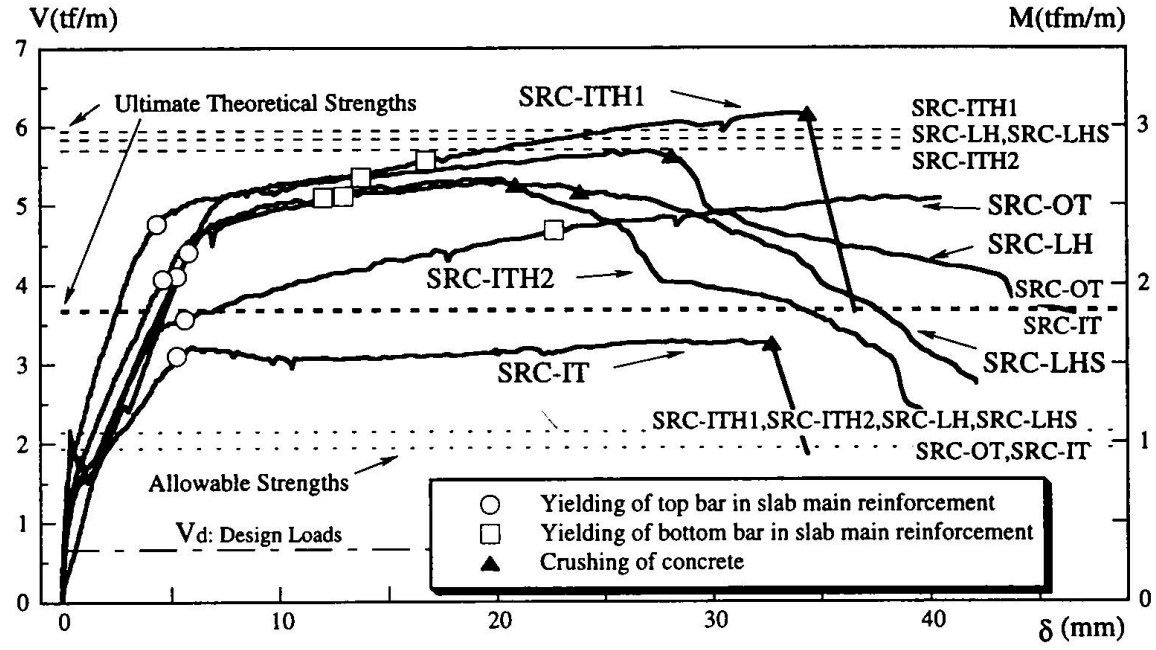

Fig. 5 Vertical load (V) versus displacement (δ) relation

Table 2 Allowable strengths and ultimate strengths

Specimens	Theoretical Predictions				Test Results	
	Allowable Strengths for Long-term Loading		Ultimate Flexural Strengths		Observed Ultimate Strengths	
	Flexure Mall [tfm/m]	Shear Vall [tf/m]	Flexure Mu [tfm/m]	Shear Vu [tf/m]	Flexure Mutest [tfm/m]	Shear Vutest [tf/m]
SRC-OT	1.07(0.86*)	2.14(1.71*)	1.95	3.89	2.65	5.30
SRC-IT			1.93	3.86	1.75	3.49
SRC-ITH1		2.34(1.87*)	2.81	6.14	2.91	6.37
SRC-ITH2			2.70	5.90	2.54	5.54
SRC-LH			2.77	6.06	2.70	5.89
SRC-LHS			2.77	6.04	2.52	5.50

* Based on specified yield strength of Re-bars(fy=3000kgf/cm^2), and design compressive strengths of concrete (f'c=270kgf/cm^2).

determined by a theory [4] are presented by dotted lines and dashed lines, respectively. In addition, the design loads (V_d) based on the current Japanese Standards are given in the figure. Each of the theoretical strengths and ultimate strengths obtained from the experiment are also listed in Table 2.

Summarizing the test results obtained;
(1). The observed ultimate strengths (V_{utest}) of all the test specimens are more than 4.1 to 7.4 times as large as the design load (V_d), and more than 1.6 to 2.7 times as large as the allowable strength for long-term loading (V_a).
(2). The ordinary T-shape Specimen (SRC-OT) could develop its ultimate flexural moment capacity (V_u) and has excellent deformability without any concrete crushing.

(3). Specimen (SRC-IT), which is the inverted T-shape specimen having the same slab reinforcing details with the ordinary T-shape Specimen (SRC-OT), could almost develop its ultimate flexural moment capacities determined by the approximate equation [4], in which Re-bars at the bottom of slabs are not taken into consideration, but was not able to develop its theoretical ultimate flexural strength (V_u). In a large deformation area, brittle shear failure occurred at the fixed end of the slabs, and then rapid deterioration in load-carrying capacity took place. This type of failure was also observed in the experiment using R/C beams and inverted T-shape and L-shape slabs specimens [2,3], but could not be expected by an existing design method such as used for designing ordinary R/C slabs with T-shape cross-section [4].
(4). The special diagonal shear reinforcements, which are provided in Specimens (SRC-ITH1), (SRC-ITH2), prevented the brittle shear failure such as observed in the Specimen (SRC-IT) and could increase their ultimate strengths considerably. Finally both specimens failed in shear failure mode in slab concrete, where shear cracks were running from the bottom of slab end toward the loading point. A minor difference of strength and ductility between these specimens would be caused by the slight difference on compressive strengths of the concrete.
(5). In Specimens (SRC-LH), (SRC-LHS), the special diagonal shear reinforcements contributed to increase the ultimate strength, and prevented the occurrence of brittle shear failure at the fixed end of the slabs in a large deformation area.

5. Concluding Remarks

In order to create a higher quality of residential environment, a SRC new apartment building with double-floor system was proposed, and some experimental studies were performed to develop the better reinforcing method for slab-to-beam connection details. From the test results, it can be concluded that the special diagonal shear reinforcements are quite effective to prevent the brittle flexure-shear failure and crushing compression-concrete in large deformation area in the slab-to-beam connection of the inverted T-shape floor slabs in SRC building structures, as well as R/C structures, and to develop the ultimate flexural strength and the large ductility.

6. References

[1] Ministry of Construction of Japanese Government. Investigation Report on Housing Demand and Problems, 1989, in Japanese.

[2] Yoshimura, K., Kikuchi, K., Kuroki, M., Yoshida, K., Iida, I. and Okita, K. Experimental Study on Strength and Ductility of R/C Suspended Slabs. Proc. of 15th Conference on Our World in Concrete & Structures, August 1990, Singapore, pp.381-388.

[3] Yoshimura, K., Kikuchi, K., Iida, I. and Okita, K. A New Building Structure with Double-floor Slab System. Proc. of the Fifth East Asia-Pacific Conference on Structural Engineering and Construction, July 1995, Australia, pp. 1845-1850.

[4] Architectural Institute of Japan. Standard for Structural Calculation of Reinforced Concrete Structures, 1988.

[5] Building Standard Law in Japan. 1994 edition.

Acknowledgment

The authors are deeply indebted to Messrs. M. Ono and Y. Matsumoto, former graduate students of Oita University, for their considerable assistance in the experiment and preparation of this paper.

CFT Beam-Column Connection with High Strength Materials

Toshiyuki FUKUMOTO
Senior Research Eng.
Kajima Corp.
Tokyo, Japan

Toshiyuki Fukumoto, born 1956, graduated from Tokyo Denki Univ. His main research interests are are composite structures, recently concrete filled steel tube structures.

Yoshikazu SAWAMOTO
Research Eng.
Kajima Corp.
Tokyo, Japan

Yoshikazu Sawamoto, born 1965, received Master degree of Eng. from Kyoto Univ. His main research interests are composite structures and connection of steel structures.

Summary
This study examined two types of CFT beam-column connections which employed high strength steel (590, 780MPa) and high strength concrete (60-120MPa). The connections have less difficulties in filling the concrete mixture in column steel tubes. One type has inner diaphragm with large opening, and the other type has external vertical stiffeners. This study employed structural tests for clarifying the structural characteristics of these connections and for developing a prediction method of ultimate load resistance of these connections.

1 Introduction

Concrete Filled steel Tube (CFT) Columns are expected high load resistance by using high strength concrete and high strength steel, and this high resistance extends to the practical application of these CFT columns to large structures such as high rise buildings. High performance building structures using these CFT columns, which employed high strength steel (590, 780MPa) and high strength concrete (60-120MPa), and steel beams have been under development by the authors. However, these structures have difficulties in filling concrete into the column steel tubes since fresh mixture of the high strength concrete is very viscous. This difficulty is aimed at being overcome by using new types of beam-column connections, which are: 1) with diaphragm having wide opening and large thickness, or 2) with vertical stiffeners outside of a column steel tube, which are installed between beam flanges to avoid interference with finishing material and reinforcement in floor slab (Fig. 1).
Similar connections have been investigated by Morita et al, but have different geometry from those connections presented herein. Furthermore, few researches have done by examining the connections with high strength constitutive materials. Therefore, the authors conducted local tension tests and shear test for the connection to clarify the elasto-plastic behavior of the connections. Moreover, a methodology for predicting load resistance of the connection is also investigated in this study.

2 Outline of Tests

The local tensile test and the shear test on the proposed beam-column connections are conducted. The specimens' geometry is classified into two types, one with diaphragm having opening (ID type) and the other with vertical stiffeners (VS type) as shown in Fig. 2 and Fig. 3, and the parameters of specimen are summarized in Tables 1, 2 and 3.
As shown in Table 1, tensile tests for ID type involve six specimens, in which experimental parameters are: diaphragm thickness, opening shape in diaphragm, width-thickness ratio of steel tube, beam-column width ratio (B/D, see Fig. 2) and steel strength. Tensile tests for VS type also comprise six

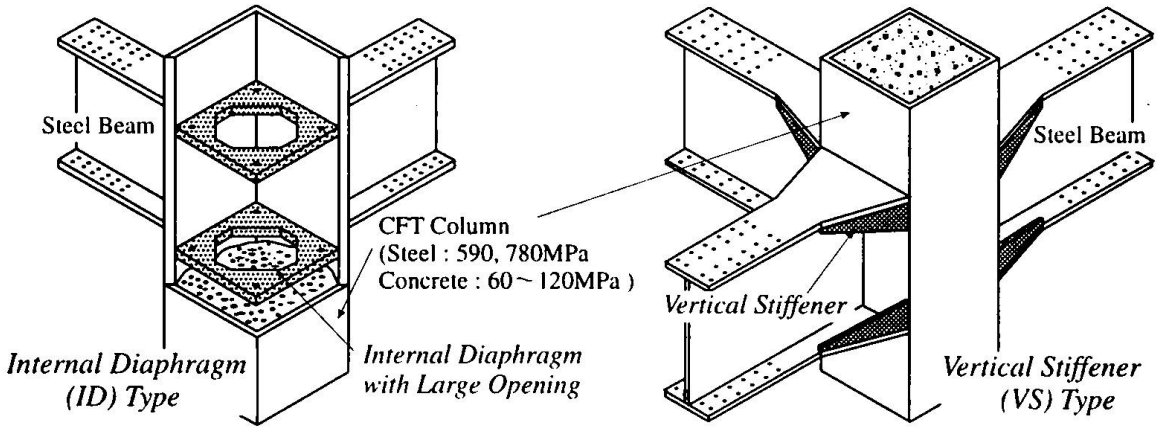

Fig. 1 Outline of Beam-Column Connection

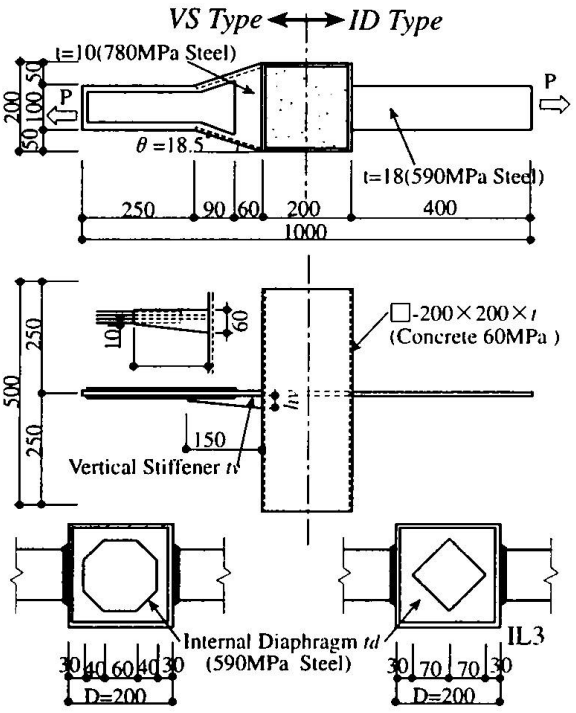

Fig. 2 Specimens of Tensile Tests

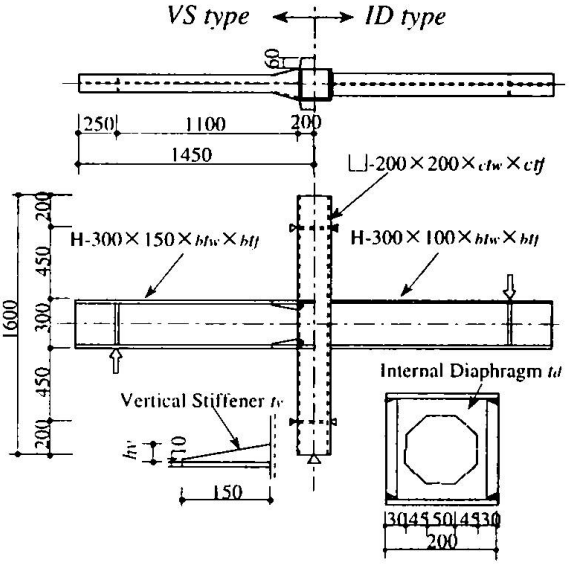

Stiffenig Type	ID type			VS type		
Specimens	IP1	IP2	IP3	VP1	VP2	VP3
ctw	6	9	8	6	6	8
ctf	9	12	12	9	9	12
btw	9	12	12	12	12	14
btf	14	14	14	19	19	25

unit: mm

Fig. 3 Specimens of Subassemblage Tests

specimens, in which experimental parameters are: stiffener height, stiffener thickness, width-thickness ratio of steel tube, and steel strength (Table 2).

Shear tests incorporate six specimens in which three specimens are ID type and the other three are VS type. Experimental parameters are steel tube's width-thickness ratio for ID type and connection panel's height-width ratio for VS type. Furthermore, steel strength and concrete strength are changed as parameters for both types of specimens. These shear tests employ common condition other than those indicated in experimental parameters (Table 3). The above tests adopted two classes of steel tube's width-thickness ratios, FA class and FC class. Steel tubes of FA class are commonly used in Japanese industry, and those of FC class have 1.5 times higher thickness-width ratio than FA class. These FC class tubes are permitted for use particularly to CFT columns while not being commonly used in the construction industry due to the vulnerability of buckling.

Tensile test specimens are rectangular CFT columns with single beam flanges, and tensile loads are applied to the ends of flange plates, as shown in Fig. 2. Shear test specimens are beam-column connections which are assumed as subassemblages composing entire frame as shown in Fig. 3. The shear force is applied to the connections through beam flanges as in this figure. Both tensile

Table 1 Specimens for Tensile Test of ID Type

Specimens		IL1	IL2	IL3	IL4	IL5	IL6
Diaphragm	Opening Shape[1]	O	O	Q	O	O	O
	Thickness *td* (mm)	9	14	9	9	9	9
Width-Thickness Ratio *D/t* (class)[2]		33(FC)	33(FC)	33(FC)	33(FC)	22(FA)	29(FC)
Strength of Steel (MPa)		590	590	590	590	590	780
Beam-Column Width Ratio *B/D*		1/2	1/2	1/2	1/3	1/2	1/2

Note 1) : O:Octago, Q:Quadrangle
2) : *D* :Depth of steel tube,*t* :Thickness of steel tube

Table 2 Specimens for Tensile Test of VS Type

Specimens		VL1	VL2	VL3	VL4	VL5	VL6
Stiffener	Height *hv (mm)*	6	6	6	14	9	7
	Thickness *tv* (mm)	30	50	50	30	30	30
Width-Thickness Ratio *D/t* (class)[1]		33(FC)	33(FC)	33(FC)	33(FC)	22(FA)	29(FC)
Strength of Steel (MPa)		590	590	590	590	590	780

Note 1) : D:Depth of steel tube, t:Thickness of steel tube

Table 4 Properties of Steel

Steel (MPa)	Thickness (mm)	σ_y (MPa)	σ_u (MPa)
590	5.6	533	689
	5.9*	514	653
	8.4	527	691
	8.9*	511	654
	13.4	572	716
780	7	836	859
	8.0*	796	854
	10	841	869

σ_y: Yield point
σ_u :Tensile strength
* : Shear tests

Table 4 Properties of Concrete

Test	σ_B (MPa)
Tensile test	57.7
Shear test	64
	116.9

σ_B :Compresive strength

Table 3 Specimens for Shear Test

Stiffenig Type	ID type			VS type		
Specimens	IP1	IP2	IP3	VP1	VP2	VP3
Width-Thickness Ratio *D/t* (class)[1]	33(FC)	22(FA)	25(FC)	33(FC)	33(FC)	25(FC)
Strength of Steel (MPa)	590	590	780	590	590	780
Strength of Concrete (MPa)	60	60	120	60	60	120
Height-Width Ratio	1.5	1.5	1.5	1.5	1.0	1.5

Note 1) : *D* :Depth of steel tube,*t* :Thickness of steel tube

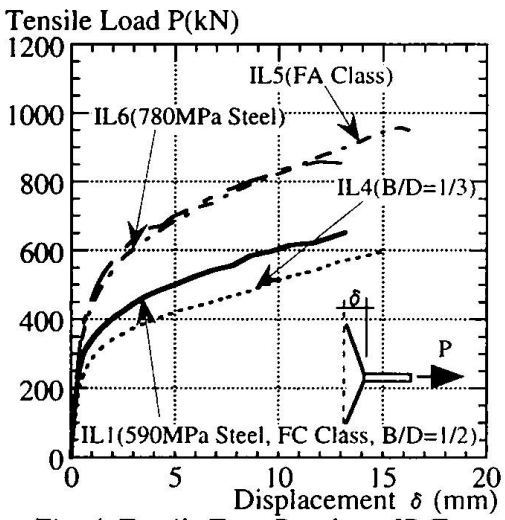

Fig. 4 Tensile Tests Result on ID Type

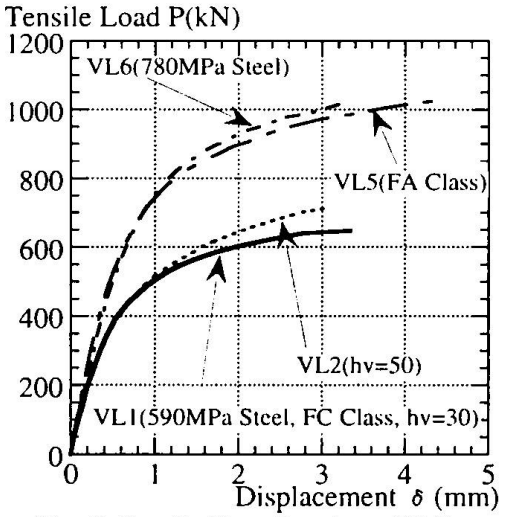

Fig. 5 Tensile Tests Result on VS Type

and shear loading are applied in monotonic manner.

3 Structural Characteristics of Local Parts of the Connections

3.1 Test Results

Tensile test results for ID type are illustrated in Fig. 4, in which load-displacement relationships are summarized. ID type specimens showed failure by crack propagation in the steel tube flange to

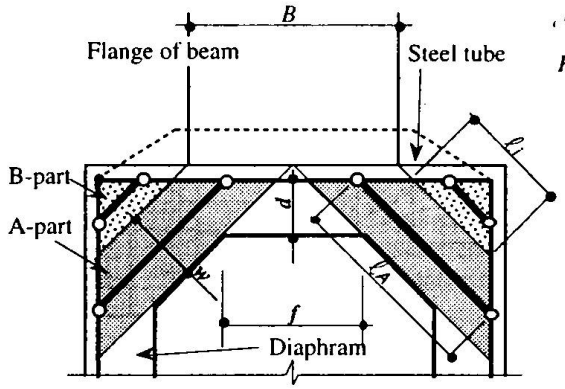

$$_cP_u = P_c + P_d$$

$$P_d = \frac{2}{\sqrt{2}}\left(W + \frac{\ell_t}{4}\right) t_d \cdot \sigma_{du}$$

$$W = \min\left(w, \sqrt{2}\frac{B}{2}\right) \quad w = \frac{1}{2\sqrt{2}}(B - f + 2d)$$

$$\ell_A = \min\left(\ell_t + W, \ell_t + \sqrt{2}\frac{B}{2}\right) \quad \ell_t = \frac{1}{\sqrt{2}}(D - B - 4t)$$

P_c :Morita's yield line theory for ultimate out-of-plane resistance of steel tube's flange[1]
t :Thickness of steel tube
t_d :Thickness of diaphram
σ_{du} :Tensile strength of diaphram

Fig. 6 Analytical Model on ID Type

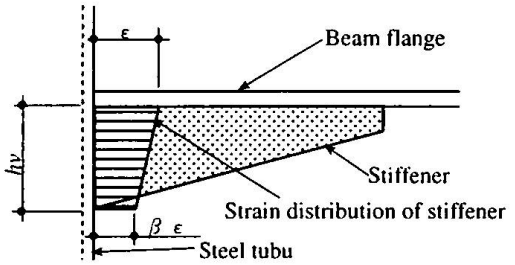

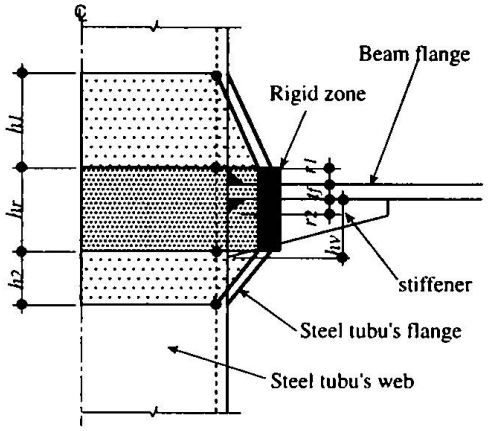

$$_cP_u = \min(P_c + P_s, P_w)$$

$$P_s = h_v \cdot t_v\left\{(1+\beta)\sigma_{su} + (1-\beta)(1-\alpha)\sigma_{sy}\right\}\cos\theta$$

$$P_w = t\left[2h_r \cdot \sigma_{wu} + \frac{2(h_1+h_2)}{3n^2}\left[\sigma_{wy} + \frac{n-1}{2}\left\{(2n+1)\sigma_{wu} + (n+2)\sigma_{wy}\right\}\right]\right]$$

$$h_r = t_f + r_f + r_2 + \kappa(h_v - r_2) \quad h_1 = x \quad h_2 = x - \kappa(h_v - r_2)$$

$$n = 1 + \frac{1}{\alpha}\left(\frac{\sigma_{wu}}{\sigma_{wy}} - 1\right) \quad \beta = 0.9 - 0.05\frac{h_v}{t_v} \quad \kappa = (1+\beta)/2$$

P_c :Morita's yield line theory for ultimate out-of-plain resistance of steel tube's flange[2]
t :Thickness of steel tube
t_v :Thickness of stiffener
x :Size of yield line theory[2]
α :Reducing rate for second slope on bi-linear modeling of stress-strain curve
θ:See Fig.2 σ_{sy}, σ_{wy} :Yield point of stiffener, tube web
σ_{su}, σ_{wu} :Tensile strength of stiffener, tube web

Fig. 7 Analytical Model on SV Type

which beam flanges were welded. In Fig. 4, load-displacement relation with different beam-column width ratio B/D is compared . Fig. 4 depicts that IL1 specimen with B/D = 1/2 shows 15 % higher yielding load and ultimate load than IL4 with B/D = 1/3. This comparison reveals that the beam width may affect load resistance of the diaphragm. Furthermore, the effects of steel tube's width-thickness ratio (IL1, IL5) and steel strength (IL1, IL6) were found to be minor on deformation capacity of local part of the connection.

Tensile test results for VS type are illustrated in Fig. 5. In these tensile tests, specimens failed by wearing of web steel at a corner of steel rectangular tube. Fig. 5 demonstrates that the specimen with high-rise stiffener (VL2) maintained greater load resistance than that with low-rise stiffener (VL1). The effect of steel width-thickness ratio (VL1, VL5) and steel strength (VL1, VL6)was also found to be minor.

3.2 Ultimate Strengths

A method is proposed to predict ultimate tensile load resistance of beam-column connection in this study. Calculation regimes in this method are represented in Fig. 6 for ID type and in Fig. 7 for VS type. In these regimes, ultimate resistance is calculated by superposing resistances of steel tube's flange and strengthening elements. This out-of-plane resistance of steel tube's flange is predicted by using so called yield line theory by Morita et al[1],[2].

Fig. 6 illustrates an analytical model in establishing formula for ID type, in which a diaphragm is assumed as diagonal braces. These braces are classified into two parts, A-part and B-part, according

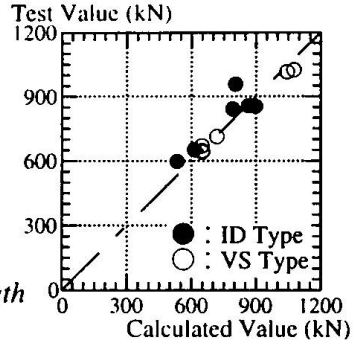

Fig. 8 Comparison in Ultimate Tensile Strength of Calculated Result and Test Result

to their resisting mechanism, in Fig. 6. This classification was adopted by analyzing the test results in which the load resistance was different depending on beam width. A-part is assumed to be directly transferred force by beams, and B-part is assumed to resist depending on the deformation of the steel tube.

Fig. 7 illustrates an analytical model for VS type, in which the stiffener is assumed as tension element with effective height. This effective height is determined by referring to the test results of strain distribution in stiffeners. By considering the fact that the failure occurred at the tube web in the tests, ultimate resistance is assumed as a smaller value of above mentioned superposition or tensile load capacity of the tube web. The prediction results using these calculation regimes were consistent with the test results. This agreement is demonstrated by the ratio of test result to the prediction result (agreement index), which is from 0.95 to 1.12 for ID type and from 0.95 to 1.04 for VS type (Fig. 8).

4 Structural Characteristics of the connection panels

4.1 Test Results

Shear test results are represented in Fig. 9 for ID type and Fig. 10 for VS type. All specimens maintained shear resistance up to 0.04 rad., and showed similar shear deformation ability independent of steel tube's width-thickness ratio, and steel strength. Shear resistance was higher for smaller height-width ratio of the connection panel. This tendency may be attributed to the difference of arch mechanism on filled concrete due to this ratio.

4.2 Ultimate Strengths

Calculated ultimate shear capacity is very conservative using the conventional formula in design guideline[3] for steel reinforced concrete structures. This tendency is demonstrated using agreement index, which is in range from1.30 to1.48 for this case (Fig. 12). Therefore, the authors proposed

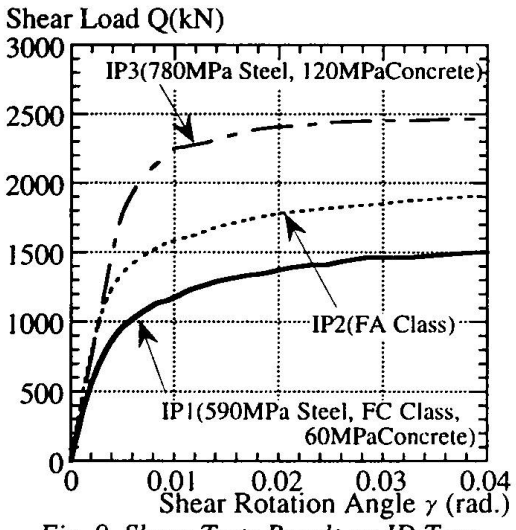

Fig. 9 Shear Tests Result on ID Type

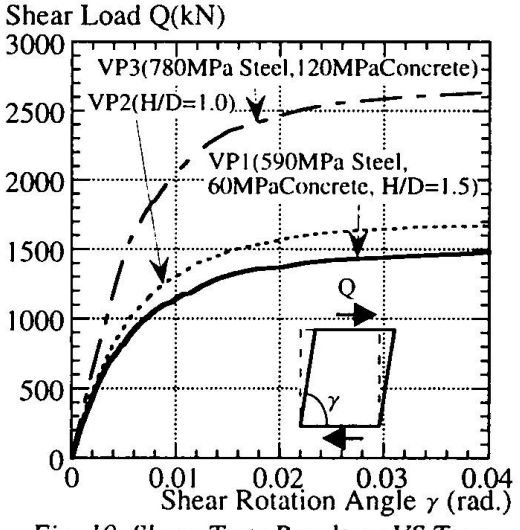

Fig. 10 Shear Tests Result on VS Type

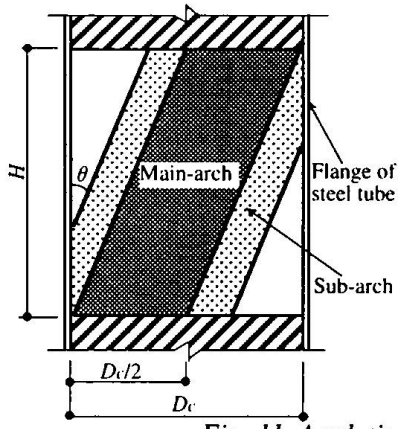

$$Q_u = Q_s + Q_c$$

$$Q_s = A_w \cdot \frac{\sigma_{wu}}{\sqrt{3}}$$

$$Q_c = \left(\frac{D_c}{2} + \frac{2}{\cos\theta} \sqrt{\frac{2M_{fu}}{t_c \cdot \sigma_B}} \right) t_c \cdot \sigma_B \cdot \tan\theta$$

$$\theta = \tan^{-1} \left\{ \sqrt{1 + \left(\frac{H}{D_c} \right)^2} - \frac{H}{D_c} \right\}$$

A_w :Section area of steel tube's web
M_{fu} :Full plastic moment of steel tube's flange
t_c :Thickness of filled concrete
σ_B :Compressive strength of filled concrete
σ_{wu} :Tensile strength of steel tube's web

Fig. 11 Analytical Model on Connection Panel

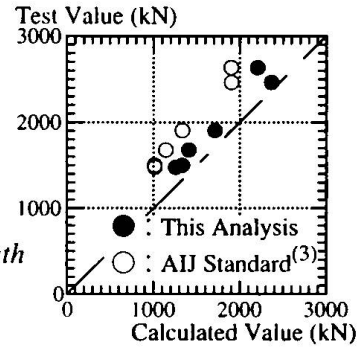

Fig. 12 Comparison in Ultimate Shear Strength of Calculated Result and Test Result

new design regime to predict ultimate shear resistance (Fig. 11). These factors have been developed under assumption that the shear resistance can be predicted by superposing the resistance of concrete and steel tube. The resistance of concrete is evaluated using arch mechanism, and that of steel is also evaluated considering only the pure shear. Two types of arch are considered, main arch by concrete itself and sub-arch by confined effect of steel tube on concrete. The contribution of the sub-arch to shear resistance was assumed to be the same as the flexural resistance of tube flange, which is calculated by assuming this flange as a cantilever. The agreement index for this regime ranged from 1.11 to 1.20 thus demonstrating good agreement between test and prediction results (Fig. 12).

5 Conclusion

a) Deformation capacity of beam-column connection was little affected by the steel tube's width-thickness ratio, steel strength (590, 780MPa), or concrete strength (60, 120MPa).
b) Ultimate tensile resistance of beam-column connection was successfully evaluated by superposing out-of-plane resistance of steel tube's flange and tensile resistance of local strengthening elements, which are assumed as simple tensile elements.
c) Ultimate shear resistance of beam-column connection was successfully evaluated using superposition of steel tube's shear resistance and concrete shear resistance, which is calculated based on arch mechanism.

References

(1) Koji Morita, Masaru Teraoka, Takahiko Suzuki : Experimental Study on Connections Between Concrete Filled Square Tubular High Strength (780N/mm^2) Steel Column and H-Beam, Proceedings of Third Pacific Structural Steel Conference, pp.591-598, 1992.8
(2) Noboru Yamamoto, Koji Morita, Hitoshi Watanabe : Effect of Stiffener on the Strength of Connection Between Beam and RHS Column, Proceedings of the Third International Symposium, Elsevier Applied Science, pp.172-179, 1990
(3) Architectural Institute of Japan : Standards for Structural Calculation of Steel Reinforced Concrete Structures, Architectural Institute of Japan, pp.44-46, 1991.9.20

Strength and Ductility of Beam-to-Column Connections in Hybrid Bridge

Shigeyuki MATSUI
Prof. Dr. of Civil Eng.
Osaka University
Osaka, Japan

Yasuyuki YUKAWA
Chief Struct. Engineer
Shikoku Branch of JH
Takamatsu, Japan

Nobuyoshi WADA
Struct. Engineer
Shikoku Branch of JH
Takamatsu, Japan

Shigeru ISHIZAKI
Manager
Sakai Iron Works Co., Ltd.
Osaka, Japan

Toshihiko TANAKA
Chief Struct. Engineer
Sakai Iron Works Co., Ltd.
Osaka, Japan

Summary

A new type of steel-concrete hybrid structure using a directly connecting method of steel girder to RC pier was employed to make the bridge behave as a structure. An elastic three dimensional finite element analysis and a static cyclic-loading test were carried out in order to confirm the ultimate strength and ductility of the connection. From those results, it was confirmed that the RC-type rigid connection employed herein is an excellent structural detail for beam-to-column connection in a hybrid rigid frame bridge.

1. Introduction

Recently in Japan, rigid frame type hybrid bridges consisting of steel girders and RC-piers have been adopted increasingly by reasons of structural simplicity and seismic advantage. In this type of bridges, it is important to design a durable and ductile structural detail for beam-to-column connections against temperature effect and earthquake.
RC-type rigid connection is a directly connecting method of steel main girder and RC pier. At the connecting section, cross beams are installed and many studs are provided on the girders and the cross beams to ensure the bond with concrete. In Okou Viaduct of Kochi-Highway in Japan, this type of connection was employed for the reasons of economical and aesthetical advantage and to obtain higher seismic resistance by increasing structural redundancy. However, until now, there is no practical construction using this type of rigid connection and the structural behaviors of the type are not clarified yet. Therefore, prior to actual construction, it is necessary to clarify the stress transfer mechanism, and to confirm the ultimate strength, the local behavior and failure, and the deformation capacity of the connection.
For the purpose mentioned above, an elastic three-dimensional finite element analysis for the connection using nonlinear joint spring elements at the interfaces of steel members and concrete was carried out. Moreover, a static cyclic loading test using a quarter scale specimen of the connection was also carried out. The paper describes the results of those analytical and experimental studies.

2. Structural Detail of Beam-to-Column Connection

The structural detail of RC-type rigid connection adopted herein is illustrated in *Fig. 1*. In this type of connection, among the stress resultant transferred from steel girder into RC pier, the major bending moment and normal force will be transferred, in the tension side of the column, mainly through the shear resistance of studs installed on the outside of web plate of the cross

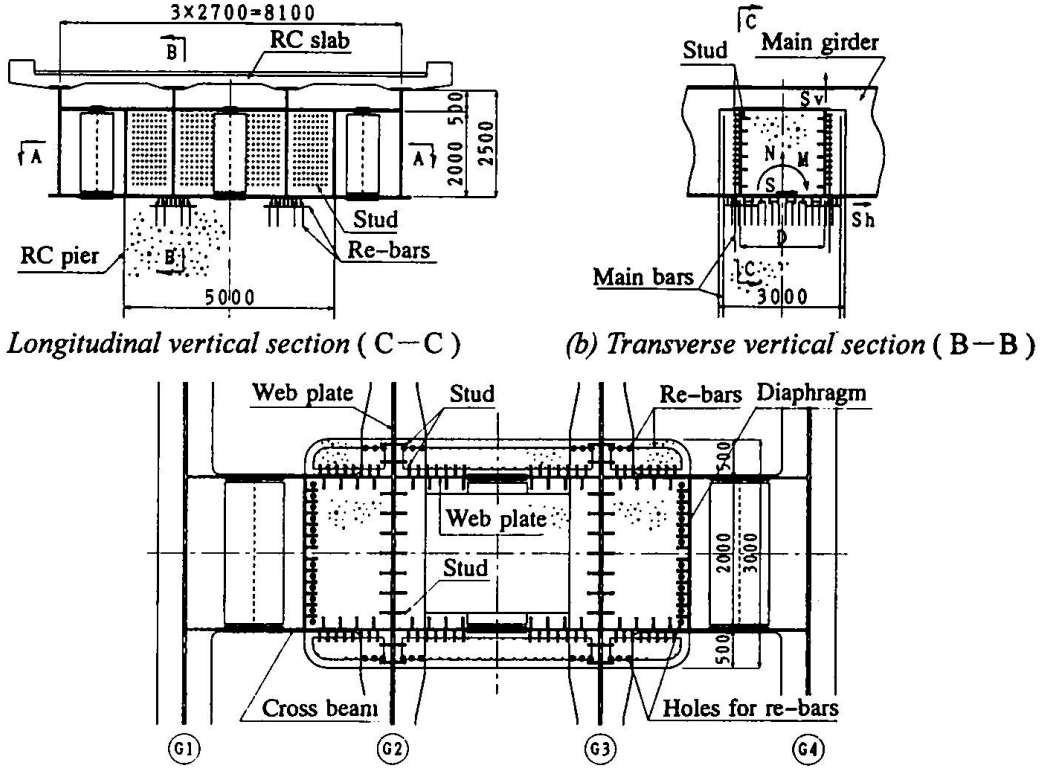

(a) Longitudinal vertical section (C—C) *(b) Transverse vertical section* (B—B)

(c) Horizontal section (A—A)

Fig. 1 Structural detail of beam-to-column connection

beam, and in the compression side, through both the shear resistance of the studs and the bearing resistance of concrete under the lower flange plate of main girders. Then the horizontal shear force will be transferred through the studs installed under the lower flange plate. Therefore, for the design of studs, it is assumed that the stress resultants from steel girders are transferred by the bearing resistance of the concrete under the lower flange and shear resistance of studs on the outside of cross beams and under the lower flange of main girder. Namely,

$$S_v = \frac{M}{D} - \frac{N}{2}, \quad \text{and} \quad S_h = S \tag{1}$$

where, S_v and S_h are the shearing forces acting on the studs on the outside of web plate of the cross beam in the tension side of the column and under the lower flange plates of main girders, respectively. M,N and S are the bending moment, axial force and shearing force acting on the column at the location of lower flange plate of main girders, respectively. D means the distance between two cross beams. In the connection, in order to transfer the shearing force smoothly to main reinforcing bars of RC pier through the studs, additional longitudinal reinforcing bars were arranged in front of the web plate of cross beams. Furthermore, the grillage reinforcement were also installed under the lower flange plate of main girders to softening the bearing stress.

3. FEM Analysis of the Connection

3.1 Analytical Model for FEM Analysis

In order to clarify the stress transfer mechanism at the beam-to-column connection through studs, an elastic three-dimensional finite element analysis for the connection was carried out with the meshing as shown in *Fig. 2*. The plate bending elements for steel girder members, the solid elements of hexahedra and pentahedra for concrete, and the nonlinear joint spring elements at the

interface of steel elements and concrete were used as finite elements of the analysis. For the boundary condition of the analysis, the each three deformations and rotations with respect to x, y and z axes were fixed at the lower bound of the concrete column. The loading on the model was given by generating the stress resultants near the connection of analytical model being equal to those for the design earthquake load of the actual bridge. Furthermore, for the spring constant of shear spring element, the results of reference[1] were used in the analysis.

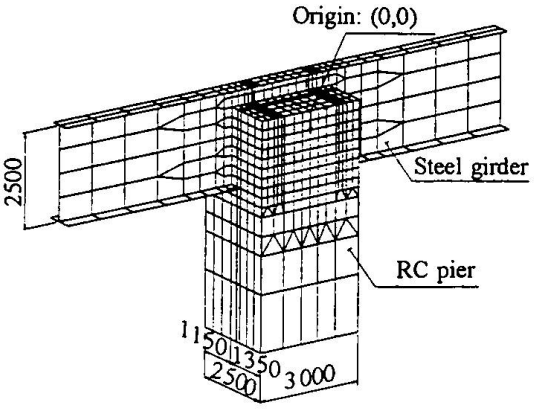

Fig. 2 Analytical model by FEM

3.2 Analytical Results and Considerations

Fig. 3 shows the distribution of shear force acting on the shear spring elements at the both outsides of web plates of the cross beams. From the figures, it can be seen that the shearing forces acting on the studs are developing larger value in the tension side than the compression side of the column. It can be considered because, in compression side, the forces from main girders are mainly resisted by the bearing of the concrete under the lower flange plate of steel girder. The shearing force per unit area given by eq.(1) is about 130tf/m^2, which is over the double of the mean value 50tf/m^2 obtained by FEM analysis. It can be explained due to the pull out resistance of studs under the lower flange plate of main girder, the bearing resistance of concrete over the flange plate, and the shear resistance of studs on the web plates of main girders

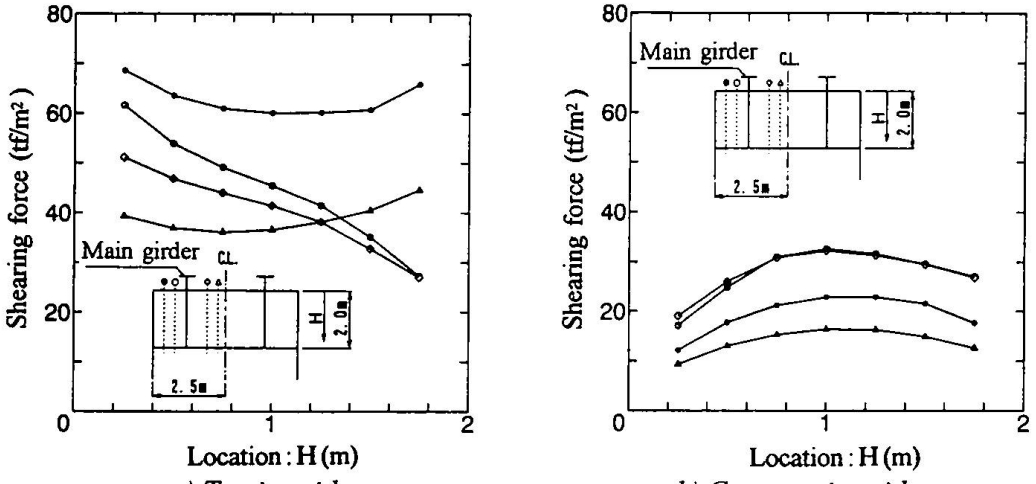

Fig. 3 Stress distribution of shear acting on studs at the outside of web plate of cross beam

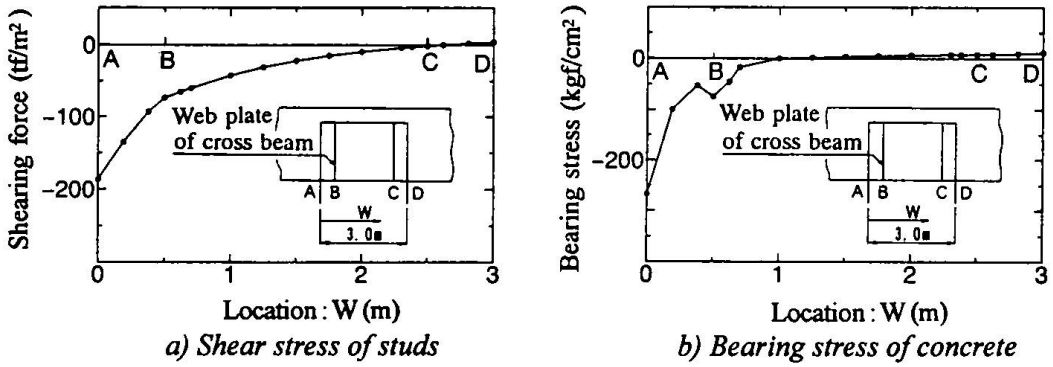

Fig. 4 Shear force distribution of studs and bearing stress distribution of concrete under the lower flange plate of main girder, respectively.

are contributing for the transmission of the resultant force in the tension side of the column. However, the eq.(1) was used for the design of studs considering that the shear strengths of studs are scattered depending on the state of the filling concrete and the shearing forces acting on studs are also scattered depending on the location. *Fig. 4* shows the distribution of the horizontal shear and the bearing stress under the lower flange plate of main girder along the web line. From the figure, it can be seen that both the shear and bearing stress acting under the flange concentrate in the edge of compression side of the column. Therefore, additional reinforcements should be installed to softening the bearing stress.

4. Static Cyclic Loading Test of Beam-to-Column Connection

4.1 Test Specimen

A quarter scale specimen of the connection with RC pier and a pair of steel main girders was employed and the specimen was installed upside down for the actual bridge from the restriction of loading equipment as shown in *Fig. 5*. Therefore, the upside-down expressions against the actual bridge are used hereafter. Moreover, the cross sectional dimensions of steel beams and the arrangement and diameter of reinforcing bars in the column were also determined to coincide with the yield moment of the complete quarter scale sections of actual bridge. The dimensions and the material properties of the specimen are shown in Table-1.

Table 1 Dimensions and material properties of the specimen

Dimensions of specimen (mm)				Yield Point (N/mm^2)	Young's Moduli (N/mm^2)
Steel Girder	Main Girder	Flange	150 x12	283	212000
		Web	625 x 9	293	211000
	Cross Beam	Flange	500 x 4.5	—	—
		Web	80 x 4.5	—	—
RC-Column	Re-bar	Main bar	D13	448	211000
		Hoop bar	D6	416	212000
	Concrete		1250x750	—	16600
Stud dowel			ϕ 13x65	—	

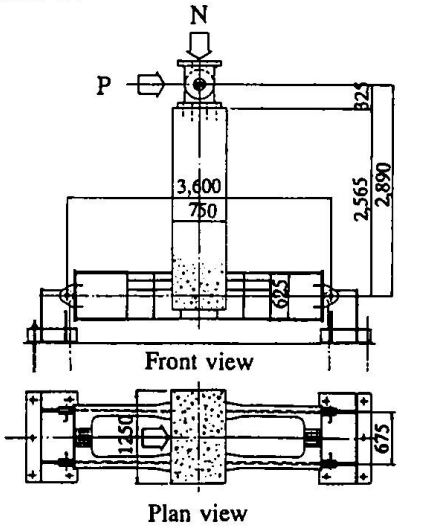

Fig. 5 General dimensions of specimen

4.2 Loading Procedure

The axial compressive load was kept in constant by vertical hydraulic actuator, while the horizontal cyclic loading was being applied simultaneously by another hydraulic jack to reproduce the same distribution of the stress resultant in the connection as actual bridge. The applied axial load was determined to give the same stresses in the specimen as the stresses in actual bridge due to dead load. Load was applied by load control method up to the initial yielding load of main bars, thereafter, displacement control method using multiples of the yielding displacement δ_y, was used. The yielding of reinforcing bar was judged by the shape of P- δ curve and the measured strain of main reinforcements.

4.3 Test Results and Considerations

4.3.1 Ultimate strength and deformation capacity of beam-to-column connection

A hysteretic curve of horizontal load versus horizontal displacement is shown in *Fig. 6*. In this experiment, the incremental displacement after yielding of reinforcements was defined by the multiples of measured initial yielding displacement δ_y. However, the displacement includes the movement of support and the displacement due to rigid body rotation of steel girder, so that the measured displacement takes apparently large value. Therefore, the revised displacement are

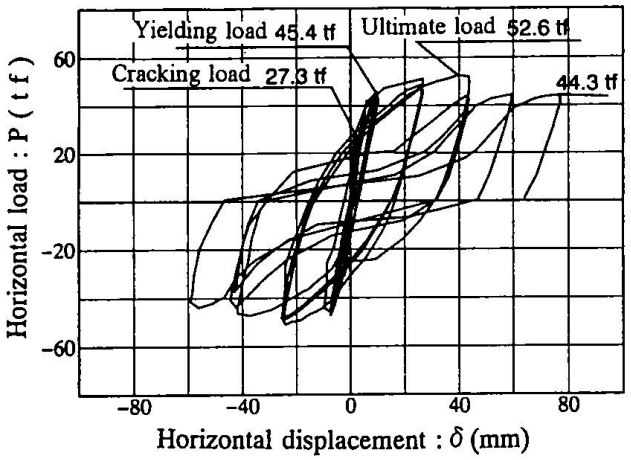

Fig. 6. Hysteretic curve of horizontal load versus displacement

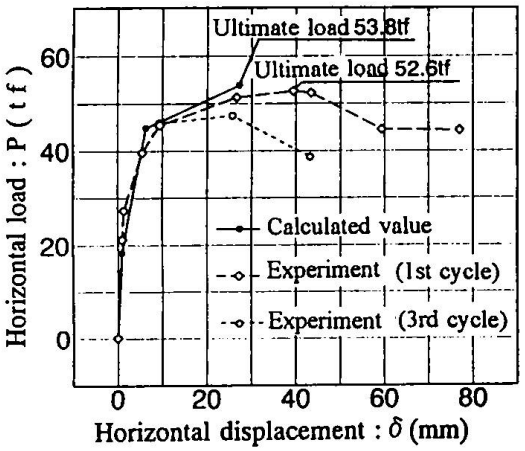

Fig. 7 Envelope of horizontal load versus displacement

Table 2 Multiples for yield displacement

Displacement	Measured	17.5	35.7	53.1	68.0	85.6
(mm)	Revised	9.4	26.6	43.4	59.4	77.0
Revised multiple number		1.0	2.8	4.6	6.3	8.2

used in *Fig. 6.* The multiple number of displacement based on revised yield displacement is shown in *Table. 2.* From these figure and table, it can be seen that the displacement for the maximum load is 4.2 times as large as δ_y and the specimen has the remaining capacity of 84% of the maximum load for the displacement of 8.2 times as large as initial yield displacement. *Fig. 7* shows the envelopes of the 1st and 3rd cycle of loading compared with a calculated value based on reference [2].
From this figure, it can be seen that, before the yielding of reinforcing bars, there is no significant difference between 1st and 3rd cycles of P- δ relation. However, after yielding of reinforcing bars, the load carrying capacity for 3rd cycle was considerably decreased comparing with that of 1st cycle. This is considered to be due to the developing of plastic region in the main reinforcements of RC column by cyclic loading. The experimental ultimate load was well agreed with the calculated one.

4.3.2 Opening between flange plate and concrete
The relationship between horizontal load and opening width of contacting surface between flange plate of main girder and concrete are shown in *Fig. 8.* Though the opening was relatively small (maximum value of 0.08mm) for the load not exceeding the cracking load of 27.3tf, thereafter, the opening rapidly increased. The maximum opening of 0.61mm was observed at the maximum load. However, for the double of design earthquake load of 21.2tf, the opening was about 0.2 mm, and no injurious cracks were observed.

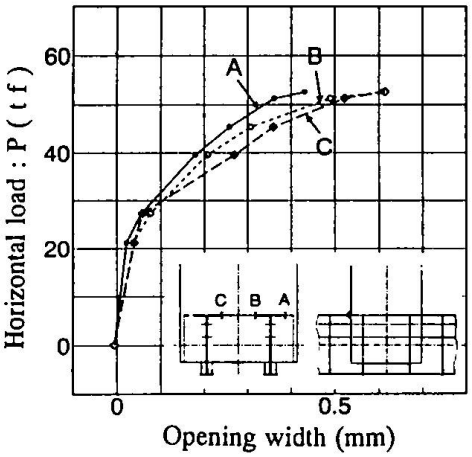

Fig.8 Opening at the contact surface of flange plates and concrete

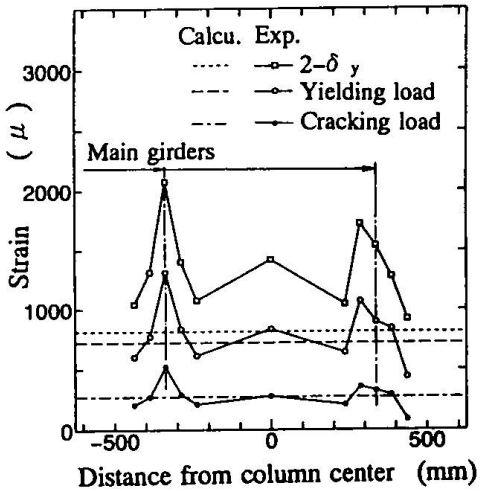

Fig.9 Strain distribution of concrete

4.3.3 Strain at the surface of concrete

Fig. 9 shows the distribution of compressive strain on the column face at the flange level of main girders for each loading level. The calculating value shown in the figure are given under the assumption of RC section ignoring tension side of concrete, and the additional longitudinal reinforcement in front of cross beams, are also taking into account in the moduli of RC section. From the figure, the bearing strain concentration can be observed over the web plate of main girder, and the test results for the cracking load was 1.9 times as large as calculating value. However, even when the final failure of specimen, any crashing of concrete at the portion was not recognized. From the fact, it can be considered that the grillage reinforcements arranged over the lower flange plate in order to softening the bearing stress worked effectively.

4.3.4 Development of cracks and failure mode

The first crack in concrete of the specimen was observed at the cross section upside 50cm from the flange plate at the loading of 27.3 tf. The location was coincident with the terminating point of additional reinforcing bars installed in front of the web plate of cross beam. Thereafter, until the horizontal load reaches 40-tf, cracks developed and widely spread with the increase of loading. However, for the load over 40-tf, though the increase of crack width was observed, new cracks didn't occurred. The first failure occurred in concrete at the compression side of the column. The failure mode was the spalling of covering concrete with the buckling of main reinforcement as shown in *Fig. 10*. Thereafter, the concrete crushing has developed to inside of reinforcing bars with the increase of loading. However, the column concrete in the connecting part has remained in sufficiently sound at the final failure state of RC column. From the fact, it can be confirmed that the combination of the studs on the outside of the cross beams, the additional reinforcements in front of them, the main reinforcement of the column, and the hoop reinforcements enclosed these reinforcements worked effectively.

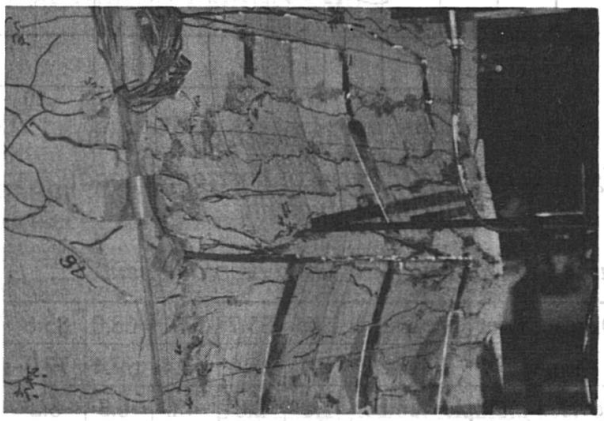

Fig. 10 Spalling-off of covering concrete

5. Conclusions

From the results of analytical and experimental studies mentioned above, the conclusions can be summarized as follows;

(1)The concrete at the connecting part was completely sound for both the principal design loads and the design earthquake load. The final failure occurred at RC column, even then the steel girder and RC pier were rigidly connected by studs.

(2)For the displacement of 8.2 times of the initial yielding displacement, the specimen has shown the remaining capacity of 84% of the maximum load carrying capacity. Therefore, it can be considered that the connection has enough ductility.

(3)The bearing strain concentration was recognized at the edge concrete of the column under the contact surface between lower flange plate of main girder and concrete. However, even when the final failure of specimen, no local failure was recognized at the part, and the connection was completely sound. From the fact, the efficacy of strengthening method adopted herein were confirmed.

References

[1] Matsuda, T., et al. : Structural Behavior of Connection between Steel Girder and RC One Using Studs, Proc. of the 50-th Annual Meeting of JSCE, I-124, Sept. 1995. (in Japanese)

[2] Japan Road Association : Reference for applying the "Tentative Specifications for Restoration of Damaged Highway Bridges by Southern Hyogo Earthquake", Feb. 1995. (in Japanese)

Bolted Connections of Hot Rolled Beams in Composite Bridges

Jingping WANG
Dr. Engineer
University of Liège
Liège, Belgium

Jingping Wang, born in 1964, Dipl.-Ing. from the North Jiaotong Univ. of Beijing in 1986, in China, Dr.-Ing. from the Univ. of Liège in 1996, in Belgium.

Raymond BAUS
Dr. Professor
University of Liège
Liège, Belgium

Raymond Baus, born in 1932, Dipl.-Ing. (1956), Dr.-Ing. (1961) from the Univ. of Liège, Head of the Dept. of Bridge and Structural Engineering at the Univ. of Liège.

Aloïs BRULS
Dr. Engineer
University of Liège
Liège, Belgium

Aloïs Bruls, born in 1941, Dipl.-Ing. from the Univ. of Liège in 1965. He is currently a research engineer in the Dept. of Bridge and Structural Eng. at the Univ. of Liège and a consultant with the company Delta G.C. in Liège.

Summary

Composite bridges with hot rolled beams, continuous on several spans, need beam splices. The position of the joint should be chosen according to the type of connections and to the moments diagrams by considering the characteristic load and the fatigue behaviour. An end plates connection by high strength bolts in composite bridges has no problem to satisfy ultimate limit states, however, the fatigue life is often limited. By comparison with several types of connections, an end plates connection should be a safe and cheap solution.

1. Introduction

It is well known that composite bridges with rolled beams may be a cheap solution in middle span bridges. High strength steels FeE460 and FeE600 permit to reach longer span [9,10]. To obtain maximum span lengths, two solutions should be envisaged. One solution considers the biggest rolled section with flange thickness not more than 40mm, HLM1100. In this case, if span length is only designed by considering ultimate limit states of the composite section steel-concrete, span length may reach 58.6 meters, for bridges with five beams in FeE460, and 61 meters, for bridges with four beams in FeE600[9,10]. For bridges with continuous beams, deflection and vibration problems arise. Bridges in steel grade FeE600 are not more interesting than steel FeE460 taking into account the limits due to deflection and vibration. Vibration and deflection conditions limit maximum span lengths, respectively to 53.5 meters and 48 meters for bridges in steel FeE460[9,10]. As this solution needs welded plates reinforcing the steel section on internal supports, fatigue life of bridges is always limited by the end of welded plates which presents much low fatigue strength. The second solution considers the rolled section HLA1100 in span and HLM1100 on the internal supports as reinforced section. In this case, a bridge with five beams in steel FeE460 may reach a span length of 51 meters, but deflection limits the span length to 42 meters. Vibrations do not limit the span length[9,10]. In the present investigation, we will consider the bridge with three beams in rolled sections HLA1100 and HLM1100. It is obvious that this solution needs a connection to splice rolled beams.

The purpose in this paper is to investigate an end plates connection by high strength preloaded bolts in composite bridges with rolled beams, satisfying ultimate limit states and fatigue behaviour. The connection position is chosen to evade the high bending moment near the internal supports and the fatigue damage. Finally, a comparison among several connections in current use is carried out.

2. Choice of the connection position

Three types of connections may be considered for beam splice. Traditional connection with cover plates and high strength friction-grip bolts(Fig.1a) may be designed anywhere along span, if it satisfies ultimate limit state. However, the connection location may be limited by the requirement of structure, economical consideration and fatigue behaviour. An end plates connection with shear studs, that has been proposed recently in composite bridges (Fig.1b), is naturally located on the internal supports[8]. For an end plates connection by bolts (Fig.1c), the location is limited in general by the characteristic load effects and fatigue behaviour. It should be chosen in function of the bending moments corresponding to the characteristic load and the fatigue loads.

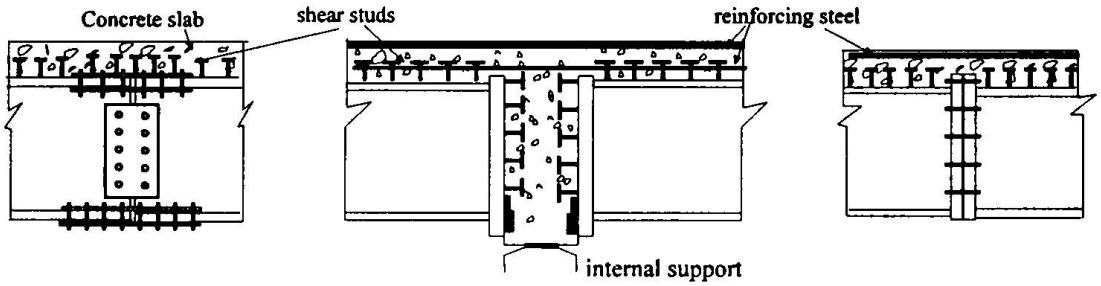

(a)Bolted cover plates connection *(b)End plates connection with shear studs* *(c)End plates connection by bolts*

Figure 1: Types of the connections in composite bridges

As an example, we treat here of a bridge with three beams, in steel grade FeE460 and two continuous spans of 32.5 meters(Fig.2). To reach this span length, the rolled section HLM1100 (FeE460) and 1.5% of reinforcing steel (S500) in concrete slab (C35/45) is foreseen on internal support. In the area of the negative bending moment, the concrete slab is considered as cracked, and do not support any tensile force. It was clear that rolled section HLM1100 should be used along the whole span to reach this span length if an end plates connection with shear studs(Fig.1b) was carried out. For other types of connections(Figs.1a and 1c), a lighter section may be acceptable in span, here, rolled section HLA1100(Fig.2). The lengths of these rolled sections may be determined by plastic moment resistance of cross section, including HLA1100 + 1.5% reinforcing steel, on the bending moment diagram given in figure 3a. Consequently, length of rolled section HLM1100 should be limited between section A and support 2(Fig. 3a). Between section C and support 2, the lower flange of the beam is always in compression under characteristic loads. The connection at section C is submitted to the lowest bending moment and the lowest shear force in the ultimate limit design, while the connection at section A corresponds to a shorter length of the reinforced section HLM1100. Considering fatigue behaviour, figure 3b shows the bending moments respectively, under fatigue loads FLM1 of Eurocode ENV1991-3 and under combination of the fatigue loads and dead loads. Between section D and support 2, the lower flange of the beam is not submitted to tension and a lower fatigue safety factor may be taken into account. Finally, the connection position should be located between section A, 1.7 m away from

support 2 and section C, 5.2 m away from support 2. But, bending moment is higher near section A, while bending moment range ΔM_f is higher near section C. Minimum bending moment range ΔM_f appears at section B, located 2.5 m away from the support 2. From section A to section B, the design moment falls down from 10000kN.m to 7720kN.m, and total reinforced length increases only 2×0.8m. The connection is finally chosen at section B.

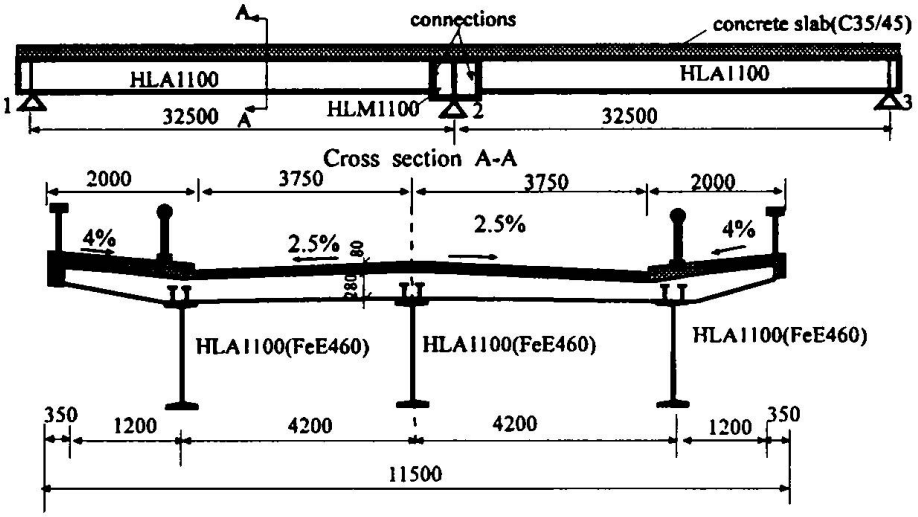

Figure 2: Composite bridge with three rolled beams

(a) Envelop of bending moment under fundamental combinaison of characteristic loads following the Eurocode-ENV1991

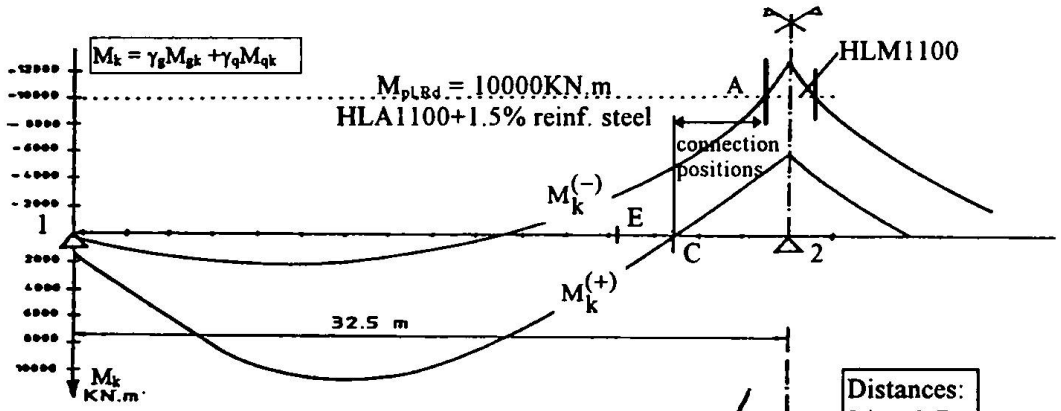

(b) Bending moment under frequent loads(FLM1) M_f and bending moment frequent loads(FLM1) + dead loads M_{g+f}

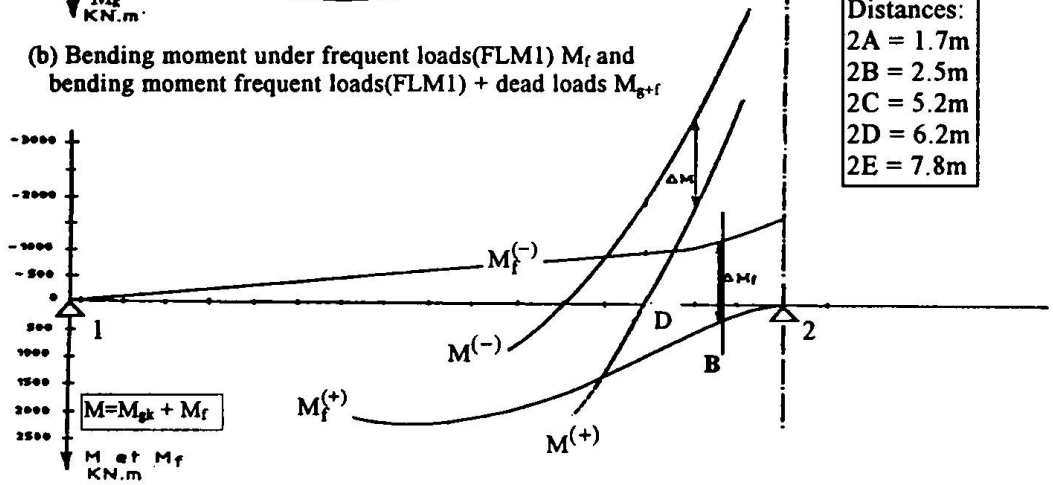

Figure 3: Bending moment diagrams

3. End-plates connection by bolts

Full penetration welds are performed between end plates and rolled beams. End plate thickness is equal to 35mm following the design method proposed by Packer and Morris[7], that is a thickness between the flanges thickness of HLA1100 (31mm) and of HLM1100 (40mm). High strength bolts M27-10.9 are used.

Design moment resistance at the connection results from three forces (Fig.4) : design tension resistance of reinforcing steel in concrete $F_{Rd,steel} = A_{s,t}f_{yd}$; design tension resistance resulted from tensile region of the connection $F_{Rd,con}$ and design resistance on compressive flange of the rolled beam $F_{Rd,comp}$. These resistance values are given in the table 1.

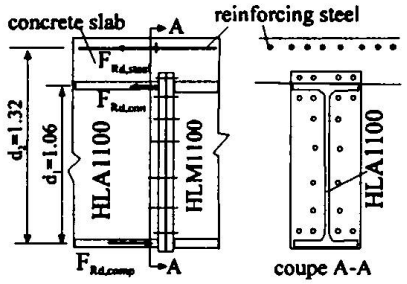

Fig.4: Ultimate resistance

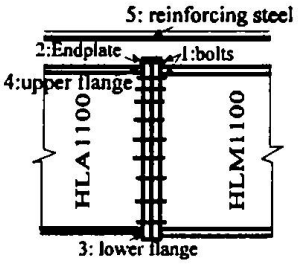

Fig. 5: Fatigue evaluations

Design tension resistance of tensile region of the connection $F_{Rd,con}$ could be determined only by considering the eight bolts close to the tensile flange, neglecting the effect of the web and another tensile bolts. That behaviour corresponds to a bolted T-stub connection for which the calculation may be performed following the method proposed in Eurocode ENV1993-1 by three possible modes of the failure. The deformation of the connection shows that the reinforcing steel reaches ultimate resistance $F_{Rd,steel}$, before the resistances $F_{Rd,comp}$ and $F_{Rd,con}$. The ultimate limit state results from the ultimate resistance of the reinforcing steel and the ultimate resistance of the flange in compression. The force in connection is below the ultimate value : $F_{Rd,com} - F_{rd,steel} < F_{Rd,con}$. As M_{Rd} is higher than the design moment M_{sd} (table 1) ultimate limit state is satisfied. Total number of bolts results from the design shear force Q_{Sd} : 20 high strength bolts of M27(10.9) are necessary(table 2).

Fatigue evaluation of the connection concerns mainly following elements in the side of section HLA1100(Fig.5) : flanges near the welds, end-plate near the weld on the upper flange, bolts in tension and reinforcing steel. The methods to determine maximum stress ranges in end plate and in bolts subject to tension and bending have been developed in elastic behaviour[10]. Fatigue life is evaluated by the method presented in the reference[1]. Fatigue strength of high strength bolts proposed in Eurocode ENV1993-1 is much lower than the value obtained by experimental results [2,5,10]. Here, we consider the fatigue strength of bolts, given in Eurocode and in the reference[10] which is similar to the one proposed in the ECSC report[2]. Fatigue evaluation results are given in the table 3. Fatigue safety factor γ_{MF}

Table 1: Ultimate moment resistance

$F_{Rd,con}$ (kN)	$F_{Rd,steel}$ (kN)	$F_{Rd,comp}$ (kN)	$F_{Rd,comp} - F_{Rd,steel}$ (kN)
2597	5888	7063	1175
$M_{Rd} = F_{Rd,steel}\, d_2 + (F_{Rd,comp} - F_{Rd,steel})d_1$ = **9016kN.m** > M_{Sd} = **7720kN.m**			

Table 2: Number of high strength bolts

	M27-10.9
M_{Sd} = 7720kN.m	8
Q_{Sd} = 1945kN	19
Total number of bolts	20

is chosen according to the values given in Eurocode. The values 1.0 and 1.35(or1.25) correspond respectively to the elements in compression and in tension. Fatigue life in

connection is governed by the lower flange near the weld (45 million cycles), this fatigue life satisfies the traffic category 2 (33 millions cycles), proposed in the Eurocode ENV1991-3.

Table 3 : Fatigue evaluation results:

	1. Bolts		2. End-plate	3. Lower flange	4. Upper flange	5. Reinforcing steel
Fatigue strength $\Delta\sigma_c$ for 2.10^6 (N/mm^2)	96 proposed value	36 value in Eurocode	71 value in Eurocode	68 value in Eurocode	68 value in Eurocode	180 value in Eurocode
Fatigue safety factor γ_{MF}	1.35	1.35	1.35	1.0	1.35	1.35
Stress range (F.L.M.1) (N/mm^2)	17.8	17.8	60.6	79.2	39.2	61.2
Stress range (F.L.M.3) (N/mm^2)	-	-	24.9	32.1	15.9	-
Fatigue life N ($\times 10^6$)	∞>133	∞>133	**46>33**	**45>33**	>133	∞>133
Traffic category	1	1	2	2	1	1

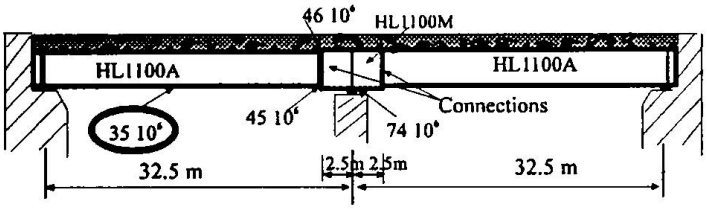

Fig 6: Results of the fatigue verification of bridge

Nevertheless, fatigue life of the whole bridge is summarised in the figure 6, in which 35×10^6 (γ_{MF}=1.25 for the element in tension) represents the fatigue life of rolled section in span and 74×10^6 (γ_{MF} =1.0 for the element in compression) represents the fatigue life of lower flange near welded stiffener on the internal support. It is clear that the end plates connection at the chosen position can offer a fatigue life (45×10^6) longer than the one governed by lower flange of the section HLA1100 in span (35×10^6). We may conclude that the connection proposed here do not limit fatigue life. In addition, to improve the fatigue life, a heavier rolled beam in stead of HLA1100 and a thicker end plate should be used.

4. Comparison with other types of connections

When an end plates connection with shear studs(Fig.1b) is envisaged, the same rolled beams HLM1100 is needed along whole span. Both, bending moment and shear force at the support, are very high and they require 48 headed shear studs (d=20mm,h=70mm) welded on the end plates for one connection and more reinforcing steel in concrete in order to transfer high bending moment on the internal support. As advantage, whole bridge needs one connection. Fatigue life in whole bridge is limited by the lower flange near the weld of the end plate to 40×10^6 cycles. This value satisfies also traffic category 2 of the Eurocode.

When a connection with cover plates and bolts is envisaged, we consider two positions, one corresponds to section B chosen for the end plates connection, and the other corresponds to the section E, located 7.8 meters away from support 2, where the number of bolts is minimum[10]. One connection with cover plates and bolts needs 108 bolts of M27-10.9 at section B, more than five times the number for an end plates connection. Fatigue life is longer than 133×10^6 (γ_{MF} = 1.0), that corresponds to the category 1 of Eurocode. The section E needs 44 bolts of M27-10.9. Fatigue life is reduced to 10×10^6(γ_{MF} = 1.25), fall down to the category 3 of the Eurocode. Total used length of rolled beam HLM1100 reaches 2×7.8 meters, in stead of 2×2.5 meters for the section B. In addition, eight cover plates at

least are needed for this type of connection, but this type of connection has no weld. A comparison among the three types of connections is given in the table 4.

Table 4 : Comparison of the three types of connections

		Number of bolts or headed studs	Number of the plates	Length of HLM1100	Weld	Fatigue life(10^6)	Category
connection by shear studs		24×2	2	65.0 m	yes	40	2
covered plate connection	position 1	108×2	8×2	5.0 m	non	>133	1
	position 2	44×2	8×2	15.6 m	non	10	3
End plates connection		20×2	2×2	5.0 m	yes	45	2

5. Conclusions

Analysis of the stress distribution of an end plates connection by high strength bolts in composite bridges with rolled beams shows that the most part of the tensile force is reported with reinforcing steel in concrete and the compressive force is transferred by the direct contact between the end plates. It is favourable to locate the connection close to the internal supports in order to obtain a short length of reinforced section. The choice of the point of an end plate connection may be deduced from the moments diagrams considering ultimate limit states and fatigue.

The present investigation shows that an end plates connection by bolts could satisfy both, ultimate limit states and fatigue behaviour. Fatigue life of an end plates connection is not shorter than the weakest one governed by details outside the connection. The end plates connection by bolts allows an important reduction of the weight of beams in comparison with the connection by shear studs and a important reduction of the number of bolts and plates in comparison with the bolted cover plates connection. The comparison among three solutions shows that an end plates connection constitutes a cheap solution.

References

1. A. Bruls, "Résistance des Ponts Soumis au Trafic Routier - Modélisation des Charges, Réevaluation des Ouvrages" Thèse de doctorat, Université de Liège, Belgium, 1995.
2. A. Bruls and E. Piraprez " Fatigue Strength of Steel Bridge" Measurement and Interpretation of Dymamic Loads on Bridges, E.C.S.C. Final report, 1995.
3. A. Bruls "Loading Effects in Modern Codes : Eurocodes" 3rd Internationalymposium on steel bridges, Rotterdam, the Netherlands, 30 Octobre -1 November,1996
4. P.J. Dowling , P.R. Knowles and G.W. Owens "Structural Steel Design" The Steel Construction Institute,1988.
5. A. Kuperus "The Fatigue Strength of Tensile Loaded Tightened HSFG Bolts" Delft University of Technology, Report 6-74-4, October 1974
6. W.H. Munse and K.S. Petersen " Rivets and High-Strength bolts - Strength in Tension" Transaction, ASCE. Vol. 126, part II, 1961.
7. J.A. Packer and L.J. Morris "A Limit State Design Method for the Tension Region of Bolted Beam-column Connections" The Structural Engineer Vol. 55, N°. 8, Aug. 1978.
8. J.B. Schleich "Acier HLE pour Ponts Mixtes à Portées Moyennes de 20 à 50 m" Report de ARBED Recherches N° 108/91.
9. J.P. Wang and A. Bruls "Composite Bridges with Hot Rolled Beams in High Strength Steel FeE460 and FeE600 upto 60 meters" RPS report N°118/92, ARBED Recherches.
10. J.P. Wang "Etude des Assemblage par Boulons Précontraints Soumis à Traction en vue de leur Application dans les Ponts Mixtes" Thèse de doctorat, Université de Liège, Belgium, 1996.